UNIVERSITY OF TWENTE.

Faculty of Engineering Technology

Modelling the Interaction among Sand Extraction, Sediment Composition, Benthic Organisms and Sand Wave Dynamics

Literature report

Wout Ploeg, MSc

February 2024

CE&M research report 2024R-001/WEM-001
ISSN 1568-4652

Literature report:

MODELLING THE INTERACTION AMONG SAND EXTRACTION, SEDIMENT COMPOSITION, BENTHIC ORGANISMS AND SAND WAVE DYNAMICS

Wout Ploeg, MSc

February 2024

Supervisors:
prof. dr. S.J.M.H. Hulscher
dr. ir. P.C. Roos
dr. ir. B.W. Borsje

Marine and Fluvial Systems
University of Twente

CE&M research report 2024R-001/WEM-001
ISSN 1568-4652

Contents

Chapter 1

Introduction

This literature review is written as part of my PhD project, which is in turn part of the NWO-funded "OR ELSE" project. This project investigates and aims to improve marine sand extraction strategies, specifically from a marine life point of view: is it possible to mitigate the negative consequences of sand extraction for sea life, and perhaps even use the extraction to create a positive impact? This project is executed with a particular focus on the Netherlands and, consequently, the Dutch part of the North Sea. Within this project, this PhD specifically focuses on the biogeomorphology of the sea bed, i.e. the coupled development of the sea bed morphology and the organisms.

To give a complete overview of the state-of-the-art research into sand wave dynamics, as well as the interaction between morphology and biology, this literature review answers the following questions:

- Q1. How do different hydrodynamical processes explain and change sand wave dynamics?
- Q2. How do sedimentological processes and sediment properties interact with sand wave dynamics?
- Q3. Which mechanisms govern the interaction between benthic organisms and sand wave dynamics?
- Q4. How does sand extraction on the Netherlands Continental Shelf influence the bed morphology, composition and benthic organisms?

Each of the following chapters will treat one of these questions and review the information required to answer it. The answers to the questions are then formulated based on the review in the conclusion (Chapter 6).

Chapter 2

Hydrodynamic Processes of Tidal Sand Waves

In this chapter, we explore the basic dynamics of sand waves: how are these features formed and modelled, and how do different physical processes influence their dynamics?

2.1 Tidal Sand Waves

Tidal sand waves (also known as tidal sand dunes) are wavy bed features, with a typical height in the order of metres, a typical wavelength in the order of hundreds of metres up to a kilometre and a migration rate in the order of metres per year. They are found worldwide in shallow shelf seas, for instance in the Southern bight of the North Sea, the Baltic Sea, the Irish Sea and the South China Sea (Van der Meijden et al., 2023) and at Long Island Sound (U.S.A.; Bokuniewicz et al., 1977). Studying sand wave dynamics is key for coastal management, as sand waves are highly dynamic and evolve on a decadal timescale. For instance, sand waves may cause navigation channels to fill up, reducing navigational depth (Campmans et al., 2021). Furthermore, sand wave migration may lead to the re-exposure of cables and pipelines and endanger the integrity of the foundations of off-shore installations (Besio et al., 2008; Németh et al., 2003).

2.2 Tidal Sand Wave Formation

Sand waves are often described as free instabilities of the sea bed, implying that they will inherently form on an (unstable) flat sea bed subject to tidal flow (Blondeaux & Vittori, 2022; Hulscher, 1996). Their formation is the result of the competition between the near-bed residual flow and the bed-slope effect (Besio et al., 2003). The residual flow (see Figure 2.1) promotes the uphill sediment transport, whilst the bed-slope effect promotes down-slope sediment transport. If the uphill transport of sediment dominates, this leads to sand wave formation due to the accumulation of sediment at the crest and the growth of the sand wave. Conversely, if the down-slope sediment transport dominates, sand waves do not form as they are dampened out (Hulscher et al., 1993).

This mechanism was postulated based on field observations by Houbolt (1968) and afterwards confirmed with a process-based modelling study by Hulscher (1996). As the residual flow is key to explaining sand wave occurrence, the vertical flow structure must be modelled explicitly to model sand wave dynamics (Hulscher, 1996). This conclusion is further confirmed by Besio et al. (2003) and Blondeaux (2001), showing that depth-averaged models (i.e. without residual flow) can only predict the occurrence of sandbanks, but not of sand waves (Hulscher et al., 1993; Vittori & Blondeaux, 2022).

As a consequence of this mechanism, a small disturbance of the bed may grow into a sand wave if the conditions allow. As the wavelength of the sand wave is not determined directly by the forcing, they are termed "free instabilities".

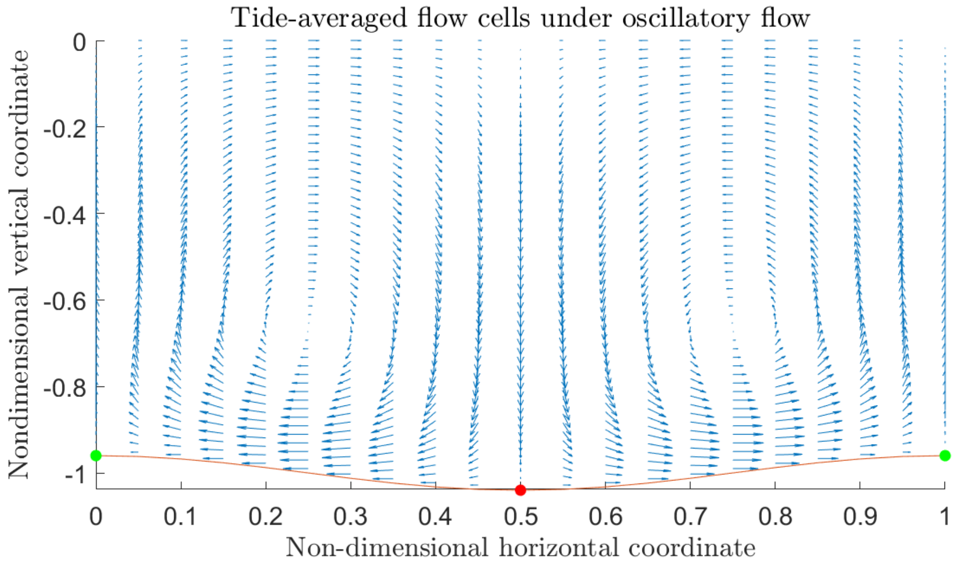

Figure 2.1: The tide-averaged flow cell over one sand wave, showing flow divergence from the troughs (red dot) and flow convergence at the crests (green dots). In case the flow is sufficiently strong to overcome the (downward) bed slope effect, sediment transport will occur in the flow direction and sediment will accumulate at the crests, leading to sand wave growth.

2.3 Sand Wave Modelling

Sand wave dynamics are often studied using process-based models to analyse the effect of specific processes and influential factors. Therefore, we briefly highlight the different modelling approaches (as also identified by Besio et al., 2008).

Complex numerical models use a detailed model, allowing for a detailed investigation of a specific area and the inclusion of a large number of processes in a detailed way. Such an approach is for instance applied by Borsje et al. (2013), Damveld et al. (2020b), and Tonnon et al. (2007) to include more processes in greater detail; Krabbendam et al. (2021) has shown that this modelling approach can be applied to acquire predictions for specific sand wave field with all site-specific details and realistic forcings. However, these approaches generally come at a large computational cost.

Non-linear idealised modelling, in which physical processes and local characteristics are omitted as much as possible, allowing for detailed investigation of a specific process. With this model, the full development of sand waves can still be computed but much faster compared to complex numerical models. The example output in Figure 2.2 illustrates this, as the computed timespan of 75 years is typically out of reach for complex numerical models. Disadvantages of this method are that a complicated solver needs to be developed (see e.g. Campmans et al., 2018; van den Berg et al., 2012) and that model studies so far tend to structurally overestimate the sand wave height (Campmans et al., 2022).

Linear idealised models also simplify the physical processes and computational domain as much as possible, but additionally assume the sand wave height to be infinitesimally small and not give feedback on the dynamics. This assumption leads to an even larger increase in the computation speed, and sometimes parts of the solution can analytically be formulated. However, the solution is only applicable for the initial formation stage of sand waves (see e.g. Campmans et al., 2017; Hulscher, 1996; Roos et al., 2001). As a consequence, only the wavelengths and orientations of the sand waves can be predicted (which this type of model can do relatively well (Campmans et al., 2022)), as well as the growth rate and possible migration rate; predicting the equilibrium height is not possible with these models.

The last strategy, also known as linear stability analysis, is explained in a bit more detail here

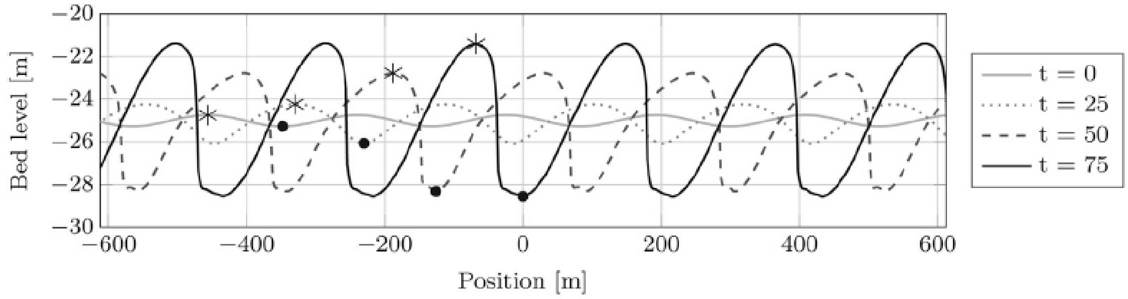

Figure 2.2: Example of the bed evolution simulated with an idealised non-linear model, showing the formation and migration of sand waves. Courtesy to van Gerwen et al. (2018).

to explain the mathematical intricacies behind this method. In this approach, one first formulates the model and derives the differential equations; in this field, this commonly yields the shallow water equations for describing the water motion, combined with a sediment transport equation and a bed-evolution equation. The gist of this modelling method is then as follows: we formulate all variables ϕ (i.e. the horizontal velocity components u or v, the vertical component w, the water level ζ, the bed level h and the sediment transport quantities) in terms of the expansion

$$\phi = \phi_0 + \epsilon\phi_1 + ..., \tag{2.1}$$

where ϕ_0 is termed the "basic state" and ϕ_1 the "perturbed state." ϵ denotes the dimensionless expansion parameter, which is the ratio of the bed disturbance amplitude to the water depth. As we assumed the sand waves to be infinitesimally small, this ratio is much smaller than one, allowing for omitting the terms of the order ϵ^2. This choice greatly simplifies the mathematics and hence reduces the computation time.

The linear stability analysis now allows us to choose an equilibrium (the basic state ϕ_0) and study the behaviour if this equilibrium is perturbed (the perturbed state ϕ_1). The meaningful equilibrium state for studying sand wave dynamics is the situation of a flat bed under a sinusoidal forcing, such that all horizontal derivatives equate to zero. However, the flat bed may be an unstable situation, in which case sand waves can grow from this state. Hence, a small perturbation upon the basic state is introduced and the evolution of this state is analysed: if the perturbation tends to grow, a pattern will emerge on the sea bed.

The linear stability analysis, therefore, aims to study the behaviour of the perturbed state ϕ_1. This is achieved by writing the evolution of the perturbed bed level h_1 as

$$\frac{\partial h_1}{\partial t} = \gamma h_1 \tag{2.2}$$

and studying the behaviour of the complex growth rate γ. This number contains the growth and decay of the amplitude (resp. positive and negative real part), as well as the migration of the bed form (imaginary part). Then, solving for the perturbed state indicates how sand waves will grow from the flat bed. By computing the complex growth rate for bed forms with different wavelengths, one can predict for every wavelength whether this mode will grow or decay, and how quickly this will happen (see Figure 2.3). The wavelength that is growing quickest is termed the "fastest growing mode" and is presumed to characterise the wavelengths of sand waves in equilibrium. The basic state is termed stable in case the growth rate for all modes is smaller than zero; if the growth rate is larger than zero for at least one wavelength, the state is unstable (Dodd et al., 2003).

2.4 Other Hydrodynamic Processes

Now that the basic processes describing sand wave formation have been reviewed, the influence of various processes on the formation and development of sand waves is discussed. This is also done with an eye on possible modelling steps taken for the research. Hence this section should also

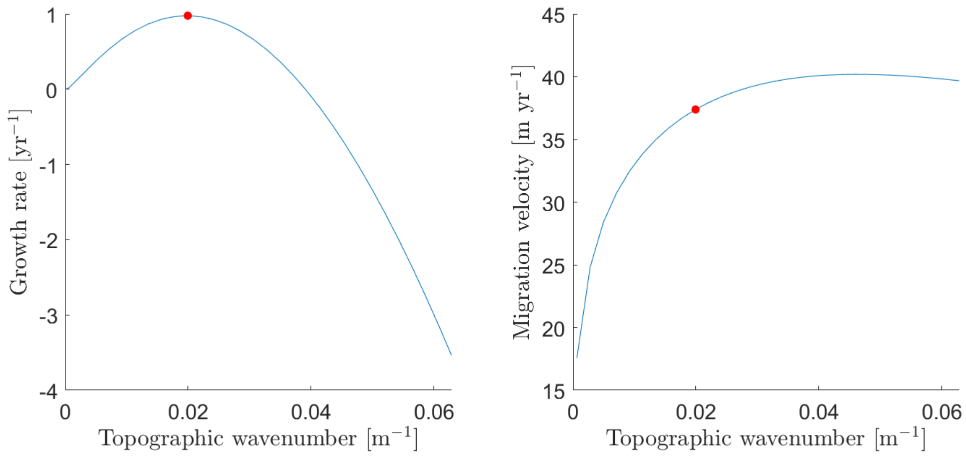

Figure 2.3: Example of the growth rate (left panel) and migration rate (left panel) as a function of the topographic wavenumber for a system under M2 tidal forcing with a small residual current. The red dot denotes the fastest growing mode.

indicate the relative relevancy of each process to allow for a substantiated decision whether (or not) to include a certain process in the model.

2.4.1 Advection of Momentum

The effect of advection on the flow patterns is key to explaining tidal sand wave occurrence because advection plays a critical role in the location of the residual current cells. This is because advection fulfils a key role in transporting the vorticity which generates the residual currents. Without advection, the vorticity would still be generated, and thus a residual current would still be present. However, the location of the flow cell would be different, which would prevent sand wave formation. This is illustrated in Figure 2.4, showing that the residual current is still present, but no longer converging at the sand wave crest and diverging at the sand wave trough. As a consequence of this, sand wave growth would no longer occur (Blondeaux, 2001; Hulscher, 1996; Hulscher et al., 1993).

2.4.2 Coriolis Effect

Whereas the Coriolis effect is of key importance in describing sand bank formation and orientation (Huthnance, 1982a, 1982b; Roos et al., 2001), it has a negligible influence on sand waves (Campmans et al., 2018; Hulscher, 1996). This is explicitly confirmed by the scaling analysis in Campmans et al. (2017). This study, however, also shows the importance of Coriolis effects in combination with for instance wind-driven flow as a consequence of Ekman spiralling. As a consequence, the near-bed flow is no longer in the same direction as the depth-averaged flow, introducing a net sediment transport orthogonal to the sand wave crest (Besio et al., 2006). To conclude: “The Coriolis effect can thus change the subtle balance between various processes.” (Campmans et al., 2017, p. 113)

2.4.3 Turbulence Closure

Different authors apply different turbulence closure models, depending on their needs and the applied models and available computational power. The work by Gerkema (2000) concludes that the eddy viscosity is an important control on sand wavelength, hence suggesting that the chosen turbulence closure influences the model outcomes.

A common assumption in linear stability analysis is the constant eddy viscosity in combination with a (partial) slip bottom boundary condition (e.g. Campmans et al., 2017; Hulscher, 1996). Hulscher (1996) has shown that such models yield qualitatively correct results, but fail to accurately describe the flow near the sea bed. This directly influences the modelled bottom-shear and thus the

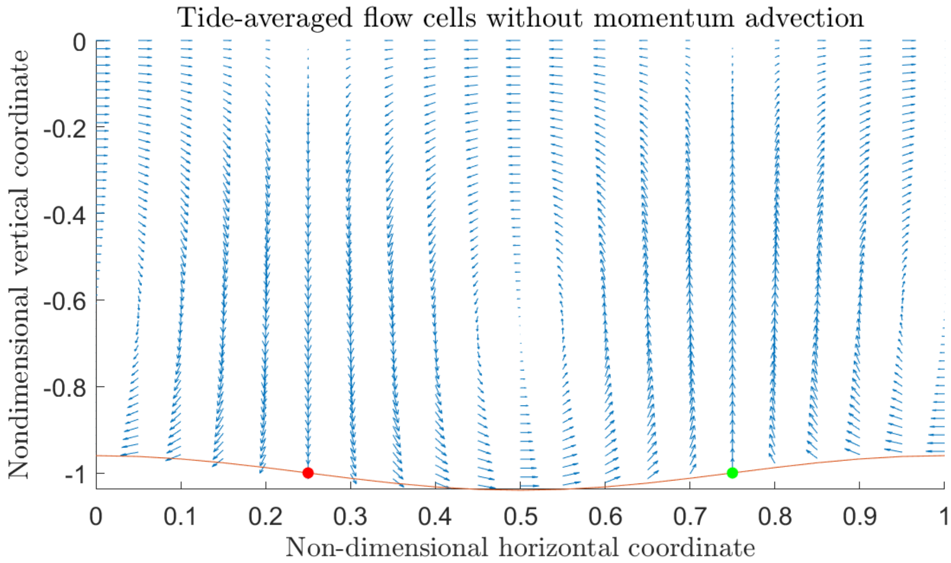

Figure 2.4: Same as Figure 2.1, but now without advection of momentum. This causes the convergence and divergence points (resp. green and red dot) to be located halfway between the troughs and crests, preventing sand wave growth.

modelled sediment transport (Besio et al., 2003). Németh et al. (2007) and Sterlini et al. (2009) show the direct influence of variations of the eddy viscosity on the sand wave patterns: a larger eddy viscosity generally leads to longer wavelengths and higher crests of the sand waves. Additionally, the choice for a constant eddy viscosity, combined with the other model assumptions, may yield the formation of sand waves with ultra-long wavelengths, much longer than observed in reality. However, it is unclear to what extent this can solely be attributed to the choice of turbulence closure and friction formulation.

To overcome these limitations, different authors proposed to allow for the eddy viscosity to vary in space and/or time. For example, Komarova and Hulscher (2000) allowed horizontal and temporal variation to account for the interaction between the bottom topography and the turbulent boundary layer. This choice can lead to the suppression of ultra-long wave-length sand waves, provided that eddy-viscosity is larger in the troughs than over the crests of the sand waves. Alternatively, Blondeaux and Vittori (2005a) introduce a formulation where the eddy viscosity is directly dependent on the distance to the bed following a Dean profile, which is consecutively applied by Besio et al. (2006) and Borsje et al. (2009a). In the Dean profile (see Fig. 2.5), the eddy viscosity equates to zero at the bed, increases to a maximum at roughly halfway through the water depth and reduces again to a nonzero value at the water surface. This allows for a more accurate representation of the vertical turbulence structure in particular closer to the sea bed, thus resulting in a more accurate approximation of the shear stress and thus of the sediment transport (Besio et al., 2003). However, this formulation is not time-dependent (although such a formulation is suggested by Blondeaux and Vittori (2005a)), hence it predicts a relatively large eddy viscosity at flow reversal. This is justified by the fact that the flow velocity is then weak, hence sediment transport will be small anyway (Besio et al., 2006; Blondeaux & Vittori, 2005a); furthermore, including a time-dependency "greatly complicates the problem and leads to similar results." (Blondeaux & Vittori, 2005a, p. 3)

A more detailed turbulence closure (e.g. the k-ϵ model by Borsje et al., 2013) can yield a much better resemblance between the modelled and observed wavelengths. However, the inclusion of the k-ϵ turbulence closure did not eliminate the growth of ultra-long wavelength features, although their growth rate was greatly reduced.

Additionally, Blondeaux and Vittori (2011) researched the importance of the horizontal diffusion of momentum, as this term is often neglected in sand wave studies. The authors showed that neglecting horizontal diffusion is justified in the case of relatively deep waters, larger grain sizes and

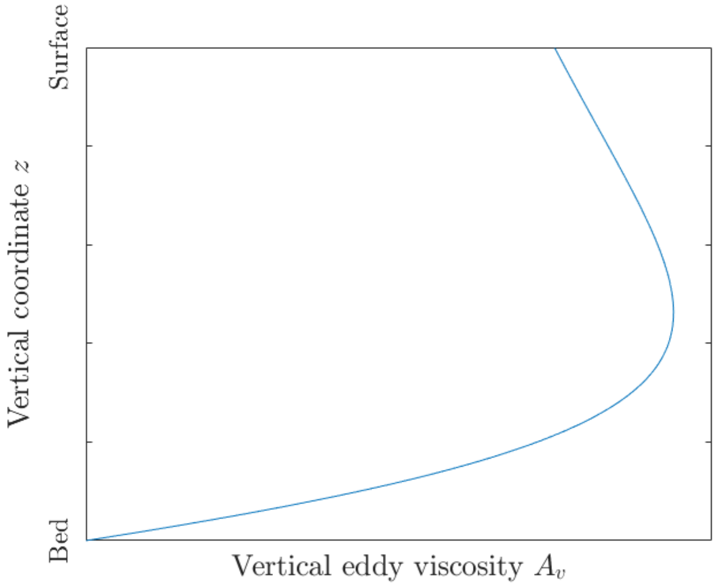

Figure 2.5: The vertical structure of the eddy viscosity following the Dean profile, as used in Besio et al. (2006) and Borsje et al. (2009a).

slower flow currents.

2.4.4 Characteristics of Tidal and Wind Forcing

In sand wave studies, the forcing is most commonly a single tidal constituent, generally the dominant M2 tide. In this section, we discuss the influence of other constituents in the forcing. It should, however, be noted that in systems that are forced with a single constituent, other constituents may be present as a consequence of the interaction between the sea bed and water motion. In this section, we solely focus on forced other constituents, not those generated due to the system dynamics.

The occurrence of a forced residual current or other tidal constituents is key for sand wave migration to occur, generally leading to sand wave migration in the direction of the residual current (Blondeaux & Vittori, 2005a; Németh et al., 2002; Roos et al., 2001). However, the combination of overtides and residual current can lead to migration against the residual current direction if the higher tidal harmonics are relatively large compared to the effect of the residual current, or in combination with a suitable phase between the tidal components (Besio et al., 2004; Blondeaux et al., 1999; Wang et al., 2019). van Gerwen et al. (2018) provide a physical explanation for the migration: the tidal asymmetry disturbs the residual flow cells, "such that convergence of sediment no longer occurs on top of the crest, but downstream of this point, which causes migration and asymmetry of the bedforms."(van Gerwen et al., 2018, p. 64). This is illustrated in Figure 2.6, showing how a residual flow to the left locates the convergence and divergence points left of the crests and troughs, hence yielding sand wave migration to the left.

Campmans et al. (2018) also relate the horizontal orientation between the residual current and tidal current to sand wave properties: the larger the angle between the two, the higher the crests and the lower the migration rate. The latter is caused by the fact that the residual flow component in the migration direction decreases, and by the fact that the sand wave height increases, as higher waves generally migrate slower (Campmans et al., 2018). It should, however, be noted that larger sand waves are still found to overtake smaller ones, which is a consequence of the influence of the larger sand wave on the hydrodynamics (Campmans et al., 2018).

It is, however, not completely clear to what extent residual currents and overtides lead to changes in sand wavelength, shape and height. Németh et al. (2002) report that the formation process and preferred wavelength are barely influenced by these. For the presence of overtides, Blondeaux and Vittori (2016) report a reduction of the wavelength with the increased presence of

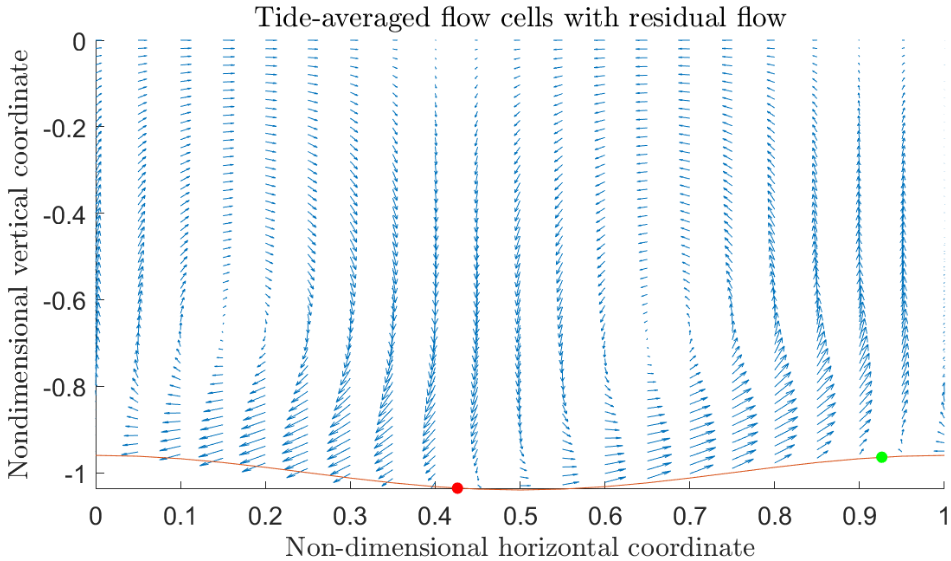

Figure 2.6: Same as Figure 2.1, but now with a residual current to the left. This causes the points of convergence (green dot) and divergence (red dot) to be located left of resp. the crests and troughs, hence causing leftward migration of the sand wave.

overtides, as well as faster migration rates and growth rates. However, both of these studies only apply to small bedforms due to the linearized models. Using nonlinear models, a reduction of sand wave height with increasing residual current velocity is found by Sterlini et al. (2009, using an idealized model) and van Gerwen et al. (2018, using a Delft3D model). Furthermore, Wang et al. (2019) report a direct relation with the wavelength: increasing residual currents yield an increased wavelength until the flow becomes too strong and a reduction in wavelength is again observed. Also Campmans et al. (2018) notice an increase in wavelength with increasing residual currents.

Blondeaux and Vittori (2010) specifically investigated the influence of the spring-neap cycle, yielding a dependency on the dominant sediment transport mode. If bedload transport was dominant, the inclusion of the spring-neap cycle accelerated sand wave formation and produced shorter wavelengths. Conversely, if suspended sediment was dominant, longer wavelengths were observed. Therefore, it seems most appropriate to qualify the specific influence of residual current and overtides on wavelength and height as largely case-specific.

Using a complex simulation model, Overes et al. (2023, 2024) showed that a realistic (non-periodic) forcing may drastically influence the properties of the sand waves, generally leading to a more dynamic sand wave pattern. This is illustrated in Figure 2.7, comparing the tide-averaged sedimentation and erosion volumes at the steep slope of a sand wave for the cases containing an M2, M4 and Z0 forcing (Case I), adding an S2 forcing (Case II) and a non-periodic time-series forcing (Case III). Figure 2.7 clearly shows that a time-series forcing, i.e. a forcing also including non-periodic components, drastically increases the variability of the sedimentation/erosion rate, and with that the migration rate of the sand wave (Overes et al., 2024). Occasionally, this even leads to migration against the dominant current direction (Overes et al., 2023). This shows a large sensitivity of sand wave dynamics on the forcing. However, this approach had a downside in that it required the time series of the boundary conditions, hence limiting the predictive capacity of the model. Furthermore, no morphological acceleration factor can be applied, due to the non-periodicity in the forcing (Overes et al., 2024).

2.4.5 Wind Waves

Depending on the conditions and the modelled sediment transport mechanism, wind waves can significantly affect sand wave dynamics. For the Belgian Continental Shelf, Durand et al. (2023) conclude that wave action can play an important role in mobilising sediment, particularly in water

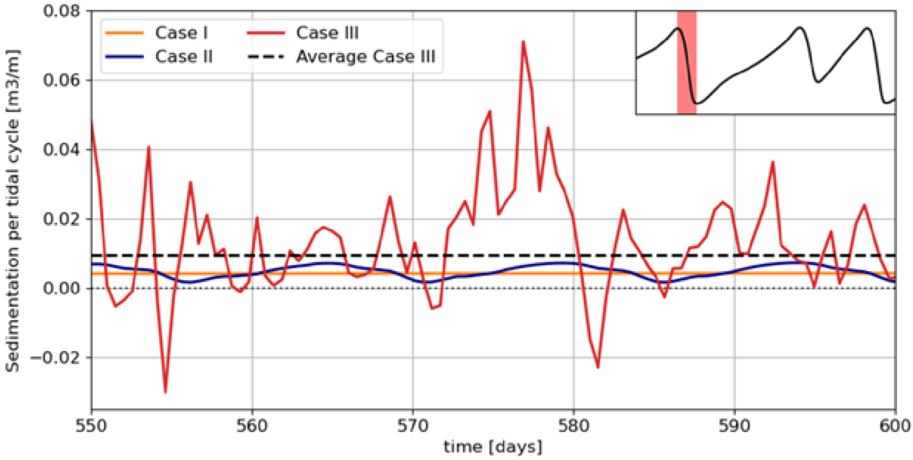

Figure 2.7: The tide-averaged sedimentation/erosion on the steep slope of a sand wave, modelled with M2, M4 and Z0 forcing (Case I), M2, M4, S2 and Z0 forcing (Case II) and with a time-series forcing including non-periodic constituents (Case III). Courtesy to Overes et al. (2024).

shallower than fifteen meters. Wind waves generally promote down-hill transport of sediment, hence leading to a reduction of the growth rate of the sand waves (Blondeaux & Vittori, 2016; Campmans et al., 2017). Furthermore, modelling studies show that wind waves reduce the sand wave height (Blondeaux et al., 1999; Sterlini-van der Meer, 2009) and increase wavelengths (Campmans et al., 2017). Furthermore, wind waves may cause, promote or reduce sand wave migration depending on the inclination of the waves to the residual current and sand waves (Campmans et al., 2017; Sterlini-van der Meer, 2009). Vittori and Blondeaux (2022) even conclude that sand waves can become flat-topped under the influence of surface waves. Finally, Sterlini-van der Meer (2009) and Van Der Meer et al. (2008) quantify the importance of a storm-induced wave climate to the general wave climate, concluding that "the relative importance of smaller wind waves coincides with observations indicating that the general wind wave climate is more important than individual large storms." (Van Der Meer et al., 2008, p. 4).

In idealised models, the effect of wind waves has often been included by superimposing the contribution of waves on the near-bed flow on the contribution by currents. This method is applied by Campmans et al. (2017, 2018) in resp. a linear and nonlinear setting. In both studies, the bed shear stress was computed as a contribution by currents and waves, with the contribution by the waves depending on the near-bed orbital velocity. This approach allows for the waves to have an impact on both the suspended and bedload transport. Sterlini-van der Meer (2009) choose a different approach by having the waves directly influence the bedload formulation. Also in complex simulation models (e.g. Tonnon et al., 2007), the contribution of waves can be included, for instance by coupling the current-model Delft3D to a wave-model like SWAN.

2.5 Formation due to Ripple Merging

A different mechanism explaining the formation of sand waves is the mechanism of pattern coarsening: small-scale features (ripples) merge into higher bedforms with longer wavelengths, ultimately becoming sand waves (e.g Duran Vinent et al., 2019; Jarvis et al., 2022). This would occur for relatively rough flows, that is $Re_d \gtrapprox 20$, with Re_d the Reynolds number based on the grain diameter. Jarvis et al. (2022) further explores this in an annular flume (see Figure 2.8), showing two different interactions between sand waves: coalescence (merging) and ejection (mass exchange without merging). Sand waves are also shown to interact over a much larger distance as a consequence of the turbulence generated by the upstream wave; turbulence from the upstream wave generates sweeps or bursts of sediment transport over the downstream sand wave, potentially even leading to repulsion between the sand waves (Bacik et al., 2020). Although it should be noted that these results are only obtained for unidirectional flow, this mechanism is rather surprising as it seems to contradict the

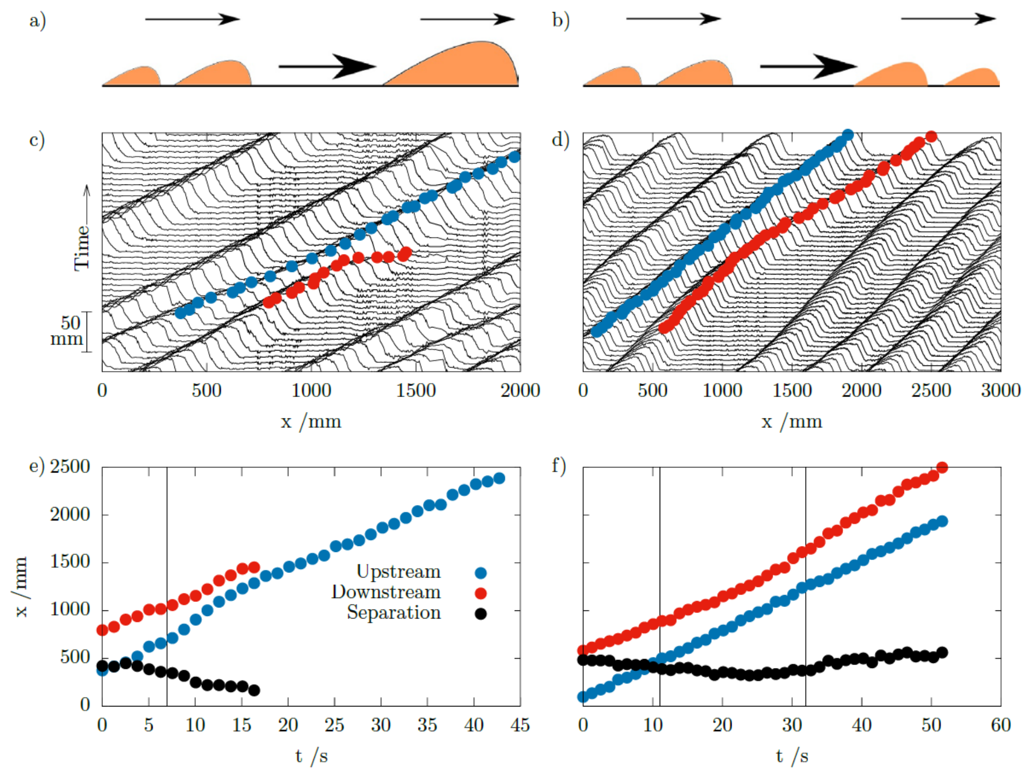

Figure 2.8: Experimental results by Jarvis et al. (2022), showing two different interactions between closely located sand waves: coalescence (merging) in the left column, where two sand waves merge into one larger one; ejection (mass exchange without merging) in the right column, where the leading (larger, slower) sand wave loses some mass to the following (smaller, faster) sand wave, such that their size and migration rates swap and the leading wave becomes smaller and faster. Courtesy to Jarvis et al. (2022).

main presumption of linear stability analyses. After all, the theory by Duran Vinent et al. (2019) postulates that ripples are forming as a result of bed instability, whilst sand waves are not; the presumption of linear stability analysis is, however, that sand waves themselves are unstable.

A few different explanations are hypothesized by the author. A first explanation could be that we falsely assume that the fastest-growing mode will also be dominant in the developed sand wave field. This would imply the fastest-growing mode depends on time. An example of this is shown by Damveld et al. (2020b), where the inclusion of benthic species induces a temporal preference for shorter wavelength sand waves; only over time, the wavelength grows to the value achieved without organisms. As ripples induce the same effect as benthic organisms (they increase bottom friction and reduce with faster flows), this could potentially indicate that the inclusion of sand ripples leads to a preference for shorter wavelengths at first, which consecutively merge into larger ones. Another explanation is that the ripples are the real-life perturbation which is added as a small bed perturbation in linear stability analysis. Another explanation could be that the ripples indeed have the largest growth rate, but that they are parametrically included in stability analyses using a slip parameter; in this way, their effect on the bottom friction is included, without explicitly simulating their presence.

Chapter 3

Sediment Transport Processes

This chapter elaborates on the influence of sedimentary processes on sand wave dynamics. We explore how different processes influence sand wave dynamics and how these processes can be modelled. We start with a general discussion of the sediments occurring on the Netherlands Continental Shelf, after which we further elaborate on the basic sediment transport processes and how this leads to bed evolution. Afterwards, we describe the most basic processes required to explain sand wave occurrence (bedload transport and the slope effect), after which we explore how different sediment properties and other processes may influence the dynamics. For those interested in the effect of sediment properties on other bedforms, we refer to Blondeaux (2012).

3.1 Sediments on the Netherlands Continental Shelf

Field observations and modelling studies suggest a strong influence of sediment properties on sand wave dynamics. Based on field data, Houbolt (1968) observed a decreasing height (and ultimately vanishing) of sand waves in the North Eastern direction in the North Sea, coinciding with a reduction in median grain size and flow velocity. The study by Van Der Veen et al. (2006) also suggests a correlation between grain size and sand wave occurrence, as their model's predictive capacity for sand wave occurrence increased when a grain size dependency was included. Creane et al. (2022) nuances this conclusion a bit, concluding based on a combined field and modelling study that not the grain size but the Rouse number (indicating bedload or suspended load dominance, and strongly correlated to grain size) is actually decisive for sand wave occurrence. If the suspended load is dominant (thus grain sizes are relatively small), sand wave growth is dampened. This is also concluded by Borsje et al. (2014) and Damen et al. (2018), also correlating the Rouse number with sand wave height and length.

Field observations also indicate variations in the grain size over an individual sand wave. Multiple authors (e.g. Cheng et al., 2020; Passchier & Kleinhans, 2005; Svenson et al., 2009) observe a sorting pattern of grain sizes: Cheng et al. (2020) report that the sediment is coarsest on the gentle slope and crest, whilst the finest fractions are found significantly more in the trough and at the lee slope, observing a variation of 25% in grain size. Svenson et al. (2009) report an increase from 350 μm in the trough to roughly 700 μm at the crest and a pattern similar to that observed by Passchier and Kleinhans (2005). Both authors also indicate a temporal variation in the grain sorting patterns: Passchier and Kleinhans (2005) indicate a general fining of the sediments in the summer period, while Svenson et al. (2009) reports variation of the sediment distribution during the tidal cycle. In modelling work by for instance Van Oyen et al. (2013), the sediment sorting is generally well predicted.

Other properties of the sediment, such as the permeability and the presence of organic compounds, may also (in)directly influence sand wave dynamics Cheng et al. (2020). The permeability generally increases with increasing grain size, as a result of which currents and waves can penetrate further in the soil, having a crucial effect on sediment nutrition and oxygen levels. Furthermore, organic compounds accumulate more in finer sediments, in particular silts and mud. As both are directly related to benthic activity, these are possible mechanisms via which grain size can (indirectly) affect the benthic communities.

On the Netherlands Continental Shelf, mud can be found at the locations where sand waves are observed, albeit only in the order of 1% mud content (Bockelmann et al., 2018). The recent (April 2023) sedimentological map of the NCS (Dabekaussen et al., 2023) also reports low percentages of mud, although their use of the Folk (1954) sediment classification implies that the mud content is somewhere between 0 and 10% in the sand wave area. Hendriks et al. (2020) reports that barely any fine sediments are found beyond 20 km offshore, although these authors also report some fines to be found in sand wave areas. If fines are found, these may also be buried below coarser sand as a result of storm activity in combination with the migration of (mega) ripples, leading to a burial depth of up to 15 centimetres (Hendriks et al., 2022). Additionally, Hendriks et al. (2020) report a profound effect of human interventions on fine sediment distribution, something that is further explored in Chapter 5 in the context of sand extraction. Low mud content can already have a distinct effect on sediment properties: at lower mass fractions, the permeability of the bed reduces whilst, at higher fractions, non-cohesive sand can become cohesive due to mud presence (Hendriks et al., 2019). Schindler et al. (2015) reports that bed forms can occur on soils with less than 10-15% mud content, which is confirmed by Bokuniewicz et al. (1977) for the case of Long Island Sound (USA). On the Netherlands Continental Shelf, sand waves are found to contain low percentages of mud (Van Dijk et al., 2012).

3.2 Process Description

Two different sediment transport modes are generally distinguished: bedload transport and suspended load transport. In bedload transport, the individual grains bounce over the bed, such that the transport is confined to a layer close to the bed. This transport occurs when the horizontal forces are sufficient to bring the sediment into motion. In suspended load transport, the lift forces (generated by the vertical velocity and turbulence) exceed the weight of the particle and it is brought into suspension. This mode of transport occurs typically higher in the water column. The joint effect of these sediment transport processes may then lead to the evolution of the bed due to erosion or deposition (Amoudry & Souza, 2011).

These basic processes may be modified by particular sediment characteristics. For instance, if a deposit consists of grains of different sizes, the larger grains may provide shelter to the smaller ones whilst the larger grains are more exposed to the flow. This may lead to increased erosion of the larger grains and decreased erosion of the smaller grains, the so-called "hiding-exposure effect" (Roos et al., 2007). Another example would be the presence of a cohesive (muddy) sediment, making the sediment more cohesive and thus more difficult to erode. Additionally, once brought in suspension, these particles may flocculate (bond together), forming larger grains and thus settling easier (Le Hir et al., 2011).

In this chapter, we explore both the basic model formulations for sediment transport, as well as the modifications to these to incorporate more advanced processes. We start with the key principle to translate sediment transport into bed evolution, after which we discuss the bedload transport mechanism. This mechanism is then extended for cases of a sloping bed, a limited sediment supply and the presence of a critical erosion stress. Then, we further highlight suspended load dynamics, after which both formulations are extended to account for mixtures of non-cohesive sediments and mixtures containing cohesive sediments.

To illustrate the effect of different processes on sediment transport, we use results by Campmans et al. (2017) as a running example in this chapter. The results are presented in Figure 3.1 and are obtained from a linear stability analysis. The results show the growth rates of sand waves of various dimensions and orientations, which are also split into the contributions from various processes. This figure will be used to illustrate the contribution of bedload transport (Figure 3.1b), which is split into the contribution by the transport itself (3.1d) and the bed slope effect (3.1f), and the contribution of suspended load transport (3.1c).

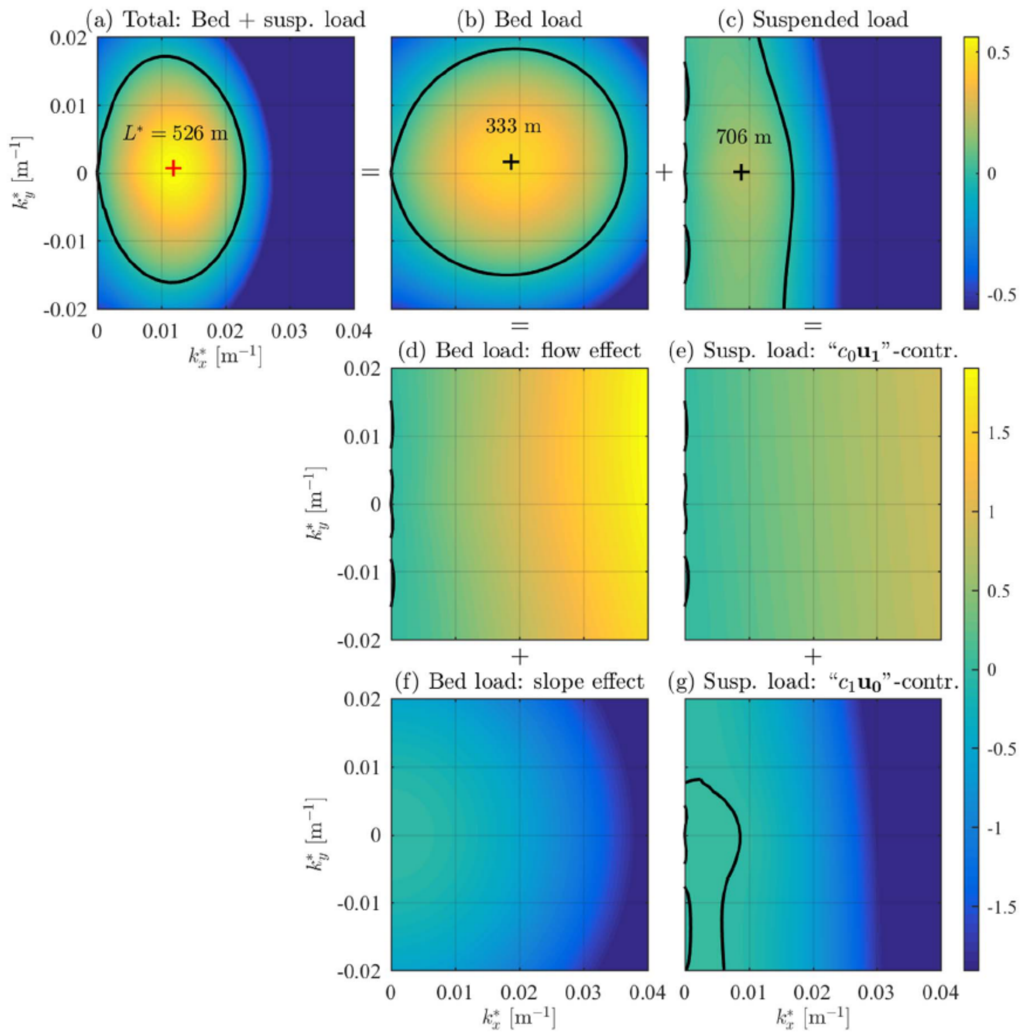

Figure 3.1: The linear growth rate [yr^{-1}] for varying topographic wavenumbers, with $k_x^* = 2\pi L_x^{-1}$ and $k_y^* = 2\pi L_y^{-1}$, with L_x and L_y the wavelengths in both horizontal directions. The different physical processes contributing to the growth rates are shown, indicating the contribution of the bedload (panel b) and suspended load (panel c). The bedload component is further split as the competition between the drag/flow effect and the slope effect. Black lines indicate the zero contour; crosses indicate the fastest growing mode. Courtesy to Campmans et al. (2017).

3.3 Bed Evolution

The bed evolution can be directly computed from the sediment transport by applying conservation of mass to the sediment, yielding the Exner (1925) equation. In its most basic form, the equation reads

$$(1-p)\frac{\partial h}{\partial t} = D - E, \tag{3.1}$$

with h the bed elevation, D and E resp. the deposition and erosion rate, and p the porosity of the deposit. Often, the combined effect of the deposition and erosion, $D - E$, is quantified as the divergence of the sediment load, i.e.

$$(1-p)\frac{\partial h}{\partial t} = -\nabla \boldsymbol{q}, \tag{3.2}$$

with $\boldsymbol{q}$ the sediment load. As the sediment transport by bedload and suspended load is often quantified with a different formulation, the total load is often split over both modes, yielding

$$\begin{aligned}(1-p)\frac{\partial h}{\partial t} &= \underbrace{D_b - E_b}_{=} + \underbrace{D_s - E_s}_{=} \\ &= -\nabla \boldsymbol{q}_b \quad - \quad \nabla \boldsymbol{q}_s,\end{aligned} \tag{3.3}$$

with subscripts b denoting bedload transport and s denoting suspended load transport.

3.4 A Basic Transport Model: Bedload

Bedload sediment transport is generally the dominant sediment transport process in sand wave areas, and consequently vital for explaining their occurrence. Although suspended load transport may also occur, the modelling study by Tonnon et al. (2007) and fieldwork by Damen et al. (2018) show that sand wave growth can only occur in areas with dominant bedload transport. This is also illustrated in Figure 3.1, showing that the bedload transport (Figure 3.1b) induces larger growth rates than the suspended load transport (Figure 3.1c). A more detailed comparison between the relevance of suspended and bedload transport is performed in Section 3.8.

Different authors apply different formulations for bedload transport, but these most commonly take the form

$$\boldsymbol{q}_b \sim \phi^n(\phi - \phi_{cr})^p \mathcal{H}(\phi - \phi_{cr}), \tag{3.4}$$

where the variable ϕ is commonly chosen as the Shields number θ and θ_{cr} the critical Shields number (Amoudry & Souza, 2011). The coefficients n and p are to be chosen, whilst $\mathcal{H}$ denotes the Heaviside function which equates to one if its argument is larger than zero, and zero if it is not. As a consequence of the definition of the Shields number, the Shields number θ depends linearly on the bed friction $\boldsymbol{\tau}$ ($\theta \sim |\boldsymbol{\tau}|$). In turn, the bed friction depends quadratically on the velocity $\boldsymbol{u}$, such that $\theta \sim |\boldsymbol{\tau}| \sim |\boldsymbol{u}|^2$. As such, the general formulation reads

$$\begin{aligned}\boldsymbol{q}_b &\sim \theta^n(\theta - \theta_{cr})^p \\ &= |\boldsymbol{\tau}|^n(|\boldsymbol{\tau}| - |\boldsymbol{\tau}_{cr}|)^p \frac{\boldsymbol{\tau}}{|\boldsymbol{\tau}|} \\ &= |\boldsymbol{u}|^{2n}(|\boldsymbol{u}|^2 - |\boldsymbol{u}_{cr}|^2)^p \frac{\boldsymbol{u}^2}{|\boldsymbol{u}^2|}.\end{aligned} \tag{3.5}$$

Following the review by Amoudry and Souza (2011), most transport equations take $n + p \approx 1.5$, a conclusion that is generally confirmed by the inventory of all bedload transport equations used in sand wave modelling, as shown in Table 3.1. This confirms that, generally, the bedload transport takes the shape $\boldsymbol{q}_b \sim |\boldsymbol{\tau}|^{1.5}$, and consequently $\boldsymbol{q}_b \sim |\boldsymbol{u}|^3$.

However, in many sand wave models, the bed-shear stress is modelled using a partial slip condition, reading

$$\boldsymbol{\tau} = \rho S \boldsymbol{u}. \tag{3.6}$$

In this formulation, the bed shear stress depends linearly on the flow velocity, implying that the equation takes a different shape than in Equation 3.5. Yuan et al. (2016, 2017) investigated the influence of a non-linear relation explicitly by taking $\boldsymbol{\tau} \sim |\boldsymbol{u}|\boldsymbol{u}$ in the context of tidal sand ridge formation, yielding no qualitative difference with a linear relation. Additionally, it should be noted that the slip parameter S also takes the dimensions of velocity. As such, it can be interpreted as a velocity, and the relation (in terms of dimensions) becomes quadratic again. As such, the majority of the formulations presented are equivalent, with the main difference being how the constants A (see Table 3.1) are defined.

3.5 A Basic Transport Model: Bed Slope Correction

An important part of the bedload transport equation is the bed slope correction to include slope-induced (downhill) sediment transport (see e.g. Hulscher, 1996). Often, a single correction term is introduced, taking the shape of

$$\boldsymbol{q}_b \sim \frac{\boldsymbol{\tau}_b}{|\boldsymbol{\tau}_b|} - \lambda \nabla h, \tag{3.7}$$

where the λ modifies the bedload transport $\boldsymbol{q}_b$ for sloping beds. The competition between the unmodified bedload transport (also called flow or drag effect) and the slope effect is shown in Figure 3.1d and f. Here, it can be observed that the flow effect always causes sand wave growth, whilst the slope effect always causes decay. Furthermore, it can be observed that shorter bed features (i.e. larger values for k_x^* and k_y^*), thus steeper slopes, increase the slope effect.

A more complicated expression has also been applied, reading

$$\boldsymbol{q}_b \sim \boldsymbol{\tau}_b - \lambda_1 \nabla h - \lambda_2 |\boldsymbol{\tau}_b| \nabla h, \tag{3.8}$$

as derived by Komarova and Hulscher (2000) and applied by Németh et al. (2007). The first term (λ_1) forms the largest correction and is related to the grain density relative to the shear stress, as well as the critical threshold of motion (if present); the second term is related to the friction angle (Németh et al., 2007). In the resulting bed profiles, including only the first term yields elongated troughs and sharper crests, while including only the second term yields smoother profiles (Németh et al., 2007). Furthermore, the slope effect is often assumed isotropic, and Yuan et al. (2016) showed that including an an-isotropic bed slope term barely changes the model outcomes.

3.6 An Extended Model: Limited Sediment Supply

Many studies investigate sand wave occurrence in areas with an abundant supply of sediment. Therefore, Porcile et al. (2017) also modelled the development of sand waves in case of limited sediment availability and concluded that this generally yields longer wavelengths compared to cases with abundant sand. Field observations in the Fehmarn Belt by Krämer et al. (2023) indicate that sand waves in sand-scarce areas are more individual features that can take complex geometries.

3.7 An Extended Model: Critical Erosion Stress

For the formulation of the bedload transport, one can choose to include a critical shear stress below which no bedload transport occurs (see e.g. Blondeaux & Vittori, 2016; Borsje et al., 2009a; Damveld et al., 2019; Van Der Meer et al., 2007; Yuan et al., 2016), or equivalently for suspended load transport (see e.g. Van Oyen & Blondeaux, 2009a). The formulation would then look like

$$\boldsymbol{q}_b \sim \mathcal{H}(|\boldsymbol{\tau}_b| - |\boldsymbol{\tau}_{cr}|), \tag{3.9}$$

with $\boldsymbol{\tau}_{cr}$ the critical bed shear stress.

Modelling studies show that an increase in the critical shear stress for bedload transport yields decreasing growth rates and wavelengths, whilst the equilibrium height is barely affected (Besio et al., 2003 for sand waves; Yuan et al., 2016, 2017 for tidal sand ridges). Furthermore, a significant drop in growth rate can be observed once the critical shear stress approaches the maximum shear

Expression	**Eqn. form** ϕ	n	p	**Sandwave studies**
Meyer-Peter-Müller:	θ	0	1.5	Besio et al. (2003)
$\boldsymbol{q}_b \sim A(\theta - \theta_{cr})^{1.5} \frac{\theta}{\|\theta\|}$				Roos and Hulscher (2003)
				Roos et al. (2005)
				Wientjes (2006)
General transport formula:	$\boldsymbol{u}$	3	0	Besio et al. (2004)
$\boldsymbol{q}_b \sim A\|\phi\|^n(\|\phi\| - \phi_{cr})^p \frac{\phi}{\|\phi\|}$				Borsje et al. (2009b)
				Campmans et al. (2017, 2018)
				Campmans et al. (2021)
				Gerkema (2000)
				Hulscher et al. (1993)
				Roos and Hulscher (2002, 2003)
				Walgreen et al. (2004)
	$\boldsymbol{\tau}$	1.5	0	Campmans et al. (2022)
				Hulscher (1996)
				Komarova and Hulscher (2000)
				Németh et al. (2002)
				Németh et al. (2007)
				Sterlini et al. (2009)
				Van Der Meer et al. (2007)
				Van Der Meer et al. (2008)
				van den Berg et al. (2012)
	$\boldsymbol{\tau}$	0	1.5	Damveld et al. (2019)
Van Rijn (1991):	θ	1.5	0	Blondeaux et al. (1999)
$\boldsymbol{q}_b \sim A(\theta - \theta_{cr})^{1.5} \frac{\theta}{\|\theta\|}$	homog. sed.			Blondeaux and Vittori (2005a, 2005b)
				Blondeaux and Vittori (2010, 2011, 2016)
				van Santen et al. (2011)
	θ	1.5	0	Blondeaux (2012)
	graded sed.			Van Oyen and Blondeaux (2009a) and Van Oyen and Blondeaux (2009b)
				Walgreen et al. (2003)
Van Rijn (2004):	θ	1	1.4	Borsje et al. (2013)
$\boldsymbol{q}_b \sim AM^{0.5}M_e^{0.7}$				Nnafie et al. (2020)
$\sim B\theta(\theta - \theta_{cr})^{1.4}$				van Gerwen et al. (2018)
Lesser et al. (2004):	u^*, T do not necessarily depend linearly on $\boldsymbol{u}$ or $\boldsymbol{\tau}$			Damveld et al. (2020b)
$\boldsymbol{q}_b \sim Au^*T$				Damveld et al. (2020a)
				Krabbendam et al. (2021)
				Leenders et al. (2021)

Table 3.1: Inventory of the different expressions used to model bedload transport when modelling sand wave dynamics. Equation form refers to the form of the equation as presented in Equation 3.4.

stress during the tidal cycle (Yuan et al., 2016). Besio et al. (2003) concludes that the inclusion of a critical shear stress yields a more realistic result and suppresses the formation of ultra-long wavelength features. For riverine dunes, an increasing critical shear stress also yields longer and lower dunes, but it is also suggested that an increased critical shear stress can account for the effect of flow separation if this is not explicitly included in the turbulence closure, as well as hiding-exposure effects (Lokin et al., 2023).

The Heaviside function is rather abrupt, which may lead to physically incorrect results and numerical issues. As such, there are different options to introduce a smoother transition between the regimes. Which option is most suitable also depends on the erosion formulation chosen. An example of this is presented by Carniello et al. (2012).

3.8 An Extended Model: Suspended Load

Although bedload transport is generally the dominant transport mode in sand wave fields, suspended load transport can still have a profound impact on sand wave dynamics. Suspended load transport is often modelled with an advection-diffusion equation (see e.g. Borsje et al., 2013; Damveld et al., 2020a), reading for example for a two-dimensional model

$$\frac{\partial c}{\partial t} + \frac{\partial (uc)}{\partial x} + \frac{\partial ((w - w_s)c)}{\partial z} = \frac{\partial}{\partial x}\left(K_{s,x}\frac{\partial c}{\partial x}\right) + \frac{\partial}{\partial z}\left(K_{s,z}\frac{\partial c}{\partial z}\right), \tag{3.10}$$

In the equation, c is the sediment concentration, w_s the settling velocity and K_s the diffusivity for various directions, which is often taken equal to the eddy viscosity (Damveld et al., 2020a). The settling velocity is usually set as a model parameter or can be determined based on an empirical relation (see e.g. Damveld et al., 2020a).

This formulation must be supplemented with appropriate boundary conditions, which are particularly relevant in the vertical direction. At the free surface, a no-flux condition is always imposed to prevent any sediment transport through this boundary. At the bed, different options are available, but the most logical option is specifying the flux at the bed as

$$\mathcal{F}_z = -(D_s - E_s), \tag{3.11}$$

with $\mathcal{F}_z$ the vertical sediment flux. The advantage of this formulation is that it directly links the suspended load to the bed evolution (see Eqn. 3.5). However, one must still specify D_s and E_s to close the system. An example of this is provided by Campmans et al. (2017), formulating the deposition as a settling process ($D_s = w_s c$) and the erosion depending on the bed shear stress ($E_s = E_s(\boldsymbol{\tau})$). A comparable, yet slightly different, formulation is the Partheniades description, prescribing

$$D_s = w_s c\left(1 - \frac{\tau}{\tau_{cr,d}}\right), \tag{3.12}$$

$$E_s = E_0\left(\frac{\tau}{\tau_{cr,e}} - 1\right)^n \mathcal{H}(\tau - \tau_{cr,e}). \tag{3.13}$$

Here, we have the background erosion E_0, n the transport power (typically 1.5), and we distinguish between a critical erosion stress for deposition ($\tau_{cr,d}$) and erosion ($\tau_{cr,e}$)) (Le Hir et al., 2011; Mengual et al., 2017).

The effect of suspended sediment transport on sand wave development is generally regarded as smaller than the effect of bedload transport, although modelling studies indicate that the contribution can still be significant (Besio et al., 2003; Blondeaux et al., 1999). The suspended load contribution is estimated to be roughly 30% of the bedload transport based on field data (Blondeaux & Vittori, 2005b). Based on their models, Borsje et al. (2014), Creane et al. (2022), and Tonnon et al. (2007) conclude that the contribution of suspended sediment transport to the total transport should not be too large, as sand waves do not occur if suspended sediment transport is the dominant transport mode. This is explained by the fact that "when suspended load transport higher in the vertical is dominant, the sediment particles can be transported beyond the crest region towards the sides of the sand wave resulting in flattening of the sand wave." (Tonnon et al., 2007, p. 258) Interestingly, Creane et al. (2022) denote that the Rouse number (the fraction between the downward settling velocity and the upward shear velocity) should not exceed 8 either, indicating a very large settling velocity relative to the flow velocity, thus very large bedload dominance. If this is the case, sand waves are not observed (Creane et al., 2022). In the context of the Belgian Continental Shelf, these results are also obtained by the modelling work by Durand et al. (2023).

The modelling study by Sterlini-van der Meer (2009) indicates that sand waves are generally lower and have shorter wavelengths when suspended sediment transport is included; this is contradicted by Campmans et al. (2017), showing that suspended load seems to increase wavelengths. The effect on the growth rate, however, seems a little more debatable: one would anticipate that an increase in the sediment transport capacity yields an increased growth rate, as found by Sterlini-van der Meer (2009), but Borsje et al. (2014) conclude that suspended sediment transport always has a damping effect on sand wave growth. It should, however, be noted that this only applies to the initial formation stage as a linear stability analysis is applied. Hence, the two conclusions do not necessarily contradict each other, as suspended sediment transport can very well reduce the growth rate in the initial formation stage, but accelerate the evolution of an existing feature, yielding faster development of the sand waves overall. Campmans et al. (2017) concludes that the effect of suspended sediment load is largely dependent on the wavelength considered, increasing the growth rates for the longer wavelengths but decreasing the growth rates for shorter features. As such, the exact effect of suspended load transport seems also largely related to the wavelength of the bed features. This effect and the competition between bedload and suspended load transport is outlined in Figure 3.1.

Finally, Borsje et al. (2014) conclude that the inclusion of suspended sediment load in combination with a k-ϵ turbulence closure model suppresses the formation of ultra-long wavelength bottom features. The use of a more complicated turbulence closure is key (Borsje et al., 2014), which aligns with the analysis by Campmans et al. (2017) where inclusion of suspended load with a constant eddy viscosity turbulence closure does not suppress the ultra-long wavelength sand waves. Another interesting development is the use of a two-phase fluid model, leaving out any distinction between bedload and suspended load transport. This approach is presented by Salimi-Tarazouj et al. (2021) and is capable of accurately modelling the merging and splitting of sand waves, yet requires an extremely fine grid and thus high computational demand.

3.9 An Extended Model: Varying Sediment Size and Grain Sorting of Non-Cohesive Sediments

Before discussing the exact effect of grain sizes on sand waves, we wish to make an important note regarding the relation between grain size and dominant transport mode. After all, finer grains are more dominantly transported by suspended load transport, whilst coarser grains are typically transported by bedload transport. Consequently, making sensible statements about the influence of grain size on model outcomes is only possible if the model contains the appropriate sediment transport mode(s) for all grain fractions.

3.9.1 Observed and Modelled Behaviour

For largely homogeneous sediment, it is known from field observations and modelling results (see e.g Blondeaux & Vittori, 2005a; Tonnon et al., 2007; Wang et al., 2019) that sand waves are no longer formed for very small or cohesive grains. For larger grain sizes in the regime for which sand waves occur, Sterlini-van der Meer (2009) and Tonnon et al. (2007) shows that grain size changes barely affect sand wave dynamics. Tonnon et al. (2007) concludes that coarser sediment particles lead to bedload dominated transport, hence net sediment transport towards the crest and thus higher sand waves; finer sediment particles yield a dominant suspended load transport, which carries particles away from the crest and thus flattens the bed. Contrary to this, van Santen et al. (2011) do find a dependency of sand wavelength on grain size, albeit only a very small positive dependency. Also Seminara (1995) and Van Oyen and Blondeaux (2009b) report a (small) damping effect on bedform growth.

These conclusions seem in line when considering a multi-modal mixture (i.e. a mixture of sediments with different grain sizes) consisting of non-cohesive sediments, as modelling studies report only marginal changes of the sand wave shape, height and wavelength when considering a bimodal mixture (Roos et al., 2007; Wientjes, 2006). However, a sorting pattern is reported in the literature, implying generally coarser sediments are deposited at the crests of the sand waves, whilst finer are generally located in the troughs. This is observed in the field by Tonnon et al. (2007) and confirmed by modelling work by Blondeaux and Vittori (2005a) and Roos et al. (2007). Van Oyen and Blondeaux (2009b) also find this trend but not for all measurement locations in the field. With a modelling study, these authors find a dependency on the strength of the tidal current: for strong currents, indeed coarsening takes place at the sand wave crests, and longer or shorter wavelengths are observed, depending on the standard deviation of the grain size mixture. For weak tidal currents, however, the fine fraction concentrates at the wave crests, and longer wavelengths are observed (in line with Wang et al., 2019). This is explained by a balance between hiding/exposure effects and reduced mobility of grains: for weak flows, the mobility of coarse grains is reduced and only fine grains accumulate at the crest. For stronger flows, "hiding/exposure effects prevail and the larger grains are found to move towards the crest." (Van Oyen & Blondeaux, 2009b, p. 338)

It should be noted that all these modelling studies concern bi-modal mixtures containing only non-cohesive sediments, solely modelled using bedload transport. In fact, no one has modelled sand wave occurrence for silt or mud, or for mixtures containing a significant percentage of these; all studies were limited to sands with a size of 62.5 μm at finest (Blondeaux & Vittori, 2005a; Van Oyen & Blondeaux, 2009a), but more commonly for sediments over 200 μm (Roos et al., 2007; Sterlini-van der Meer, 2009; Tonnon et al., 2007).

3.9.2 Modelling Layers

To model the influence of different sediment fractions, the layering of the deposit is also to be included to come to an accurate schematisation. This can include a Hirano (1971) approach for linear models, implying one active layer with a constant thickness is considered, and one substrate (see e.g. Roos et al., 2007; Walgreen et al., 2003; Walgreen et al., 2004). For non-linear models, this would not suffice and multiple layers are to be included, for instance applied by Damveld et al. (2020a). As this is the general case of a one-layer approach, we here explain the multiple-layer approach in more detail.

As an example, we take a four-layer case, from top to bottom being the active layer, layer 1, layer 2 and the substrate (see Figure 3.2). It is presumed that the active layer contains all the sediment directly available for transport, hence this layer is not just a numerical construct. Some authors, therefore, argue this layer has a thickness in the order of 2-5 D_{50} (Roos et al., 2007; Walgreen et al., 2003), others take the ripple height in the order of 10-20 centimetres or in the order of 1 meter (Damveld et al., 2020a). Importantly, this layer has a constant thickness L_a. The layers below, with thicknesses L_1, L_2 and L_s respectively, are allowed to vary in thickness. However, the thickness L_1 and L_2 have a maximal value of L_{max}; the substrate layer has no maximal thickness. Furthermore, for each of the layers, the volume fraction of the grain sizes F_i is known, such that

$$\sum_i F_i = 1 \text{ for all layers.} \tag{3.14}$$

Based on these presumptions, the following algorithm is applied by Damveld et al. (2020a) to model the development of the layered multi-modal bed:

1. For each grain size class i, determine the potential sediment transport for all transport modes, i.e. the transport in case the full top layer was made up of this grain size.
2. Compute the actual transport by multiplying the potential transport rate with the sediment availability in the top layer, yielding $q_{b,i}$ and $q_{s,i}$, the actual mass-based bedload and suspended load transport for each grain class.

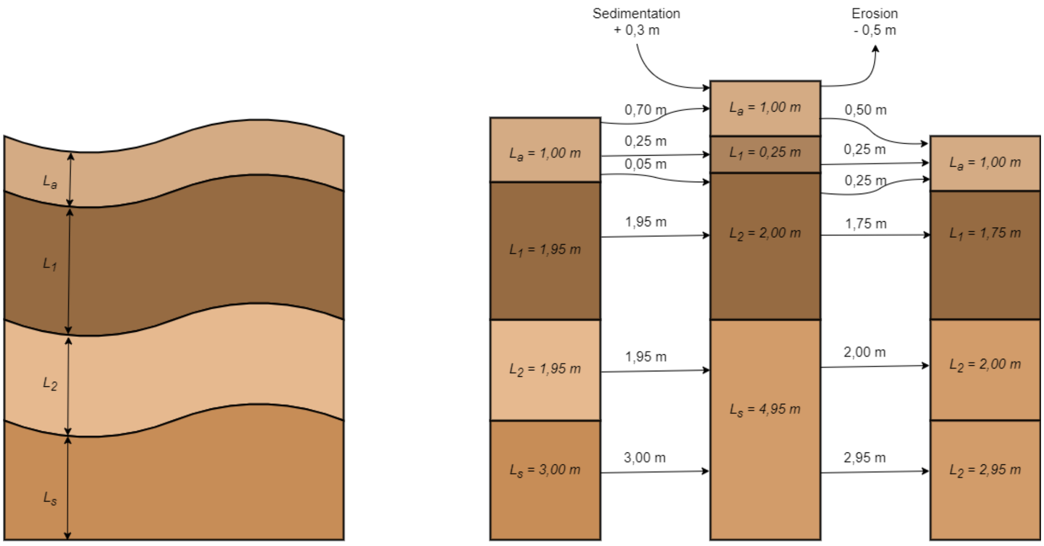

Figure 3.2: Illustration of the multi-layer approach and how deposition and erosion result in changes in the layer composition. The maximal layer thickness L_{max} for this example is taken to be 2 metres.

3. Update the bed level following

$$(1-p)\rho_s \frac{\partial z_b}{\partial t} = -\nabla \cdot \left(\sum_i q_{b,i} + q_{s,i} \right), \tag{3.15}$$

   to obtain the new bed level elevation. This is an extension of the Exner (1925) equation to a multi-modal deposit.

4. Update the composition of all layers, as well as the thickness of all but the top layer. This is done based on the following rules, also illustrated in Figure 3.2:
   - Deposition leads to a sediment flux from the active layer towards the deeper layers; if this causes the thickness of the top underlayer to exceed the maximal thickness, a new layer is created whilst the bottom layer is merged with the substrate.
   - Erosion leads to a flux from the top underlayer to the active layer. If this causes the top underlayer to disappear, the process continues with the next layer and the substrate is split to obtain the correct number of layers.
   - All layers are presumed to be well mixed.

3.9.3 Modelling Multi-Modal Sediment Transport

Two key processes play a role when considering multi-modal sediment transport. First, the erosion of sediments may be influenced by the presence of different grain sizes, as larger grains provide shelter to smaller grains, whilst the larger grains themselves are more exposed. This effect is termed the “hiding-exposure effect” and directly influences the mobility of the bed. As such, it directly influences the bedload transport formulation, as well as the erosion formulation for the suspended load transport. Secondly, the presence of multiple fractions may influence the settling behaviour of the sediments in suspension, as the presence of the grains in suspension might slow down the settling behaviour. This effect is termed “hindered settling” and directly modifies the settling velocity as used for computing suspended load transport.

To include the hiding-exposure effect, we distinguish two flavours. First, one may use a transport formulation that explicitly allows for varying grain size. An example of this is Roos et al. (2007), who use a modified version of the Meyer-Peter & Müller equation, which unmodified already allows for a dependency of the sediment transport on the grain size. Secondly, one may use a transport formulation that does not allow for this dependency and include the hiding-exposure effect as a correction. This method is applied by e.g. Damveld et al. (2020a) and Walgreen et al. (2003), Walgreen et al. (2004), who correct the Shields number θ_i for hiding-exposure. This yields the modified Shields number for each fraction ($\theta_{i,m}$)

$$\boldsymbol{q}_{b,i} \sim \theta_{i,m}^n, \; \theta_{i,m} = \xi_i \theta_i, \tag{3.16}$$

with ξ_i the hiding exposure correction and $\boldsymbol{q}_{b,i}$ the bedload transport for each fraction. Another example is provided by Roos et al. (2007) and Wientjes (2006), who include this effect by correcting the critical Shields number $\theta_{i,cr}$. This works equivalently to the critical shear stress, such that

$$\boldsymbol{q}_{b,i} \sim (\theta_i - \theta_{i,cr,m})\mathcal{H}(\theta_i - \theta_{i,cr,m}), \; \theta_{i,cr,m} = \xi_i \theta_{i,cr}. \tag{3.17}$$

Here, the critical Shields number is still to be determined and can for instance be imposed by the equation by Soulsby (1997). However, the same correction can be applied on the critical shear stress with the same correction functions, as applied in Deltares (2023); this reference also contains multiple formulations for the hiding exposure correction ξ_i (see section 11.4.3).

To include hindered settling, the effect of the grain size on the settling velocity has to be included, see for instance Damveld et al. (2020a) or Deltares (2023, section 11.3.1). The settling velocity for each fraction $w_{s,i}$ is then computed as

$$w_{s,i} = w_{s,i,0} \left(1 - \frac{\sum_i c_i}{c_{ref}}\right)^5, \tag{3.18}$$

with $w_{s,i,0}$ the uncorrected settling velocity for fraction i, c_i the concentration of fraction i and $c_{ref} = 1600$ kg m^{-3} (Damveld et al., 2020a; Deltares, 2023).

3.10 An Extended Model: Including Cohesive Sediment

3.10.1 Introduction

Including a cohesive fraction in a sand wave model is challenging due to its cohesive properties. Due to these properties, the presence of cohesive sediment also alters the properties of the non-cohesive sediment, for instance, the erosion and shear stress parameters of the soil. This interaction between the grains makes the inclusion of cohesive sediment particularly challenging compared to non-cohesive sediment, which does not show this behaviour.

We distinguish different fractions of cohesive sediment. The finest grains are termed clay and have a diameter smaller than 4 μm. Slightly larger are the silts, which are sized between 4 μm and 64 μm[1]. The combination of these two fractions is termed mud, which in turn is equivalent to cohesive sediment.

3.10.2 Effect on Sand Waves

Field measurements do indicate the existence of sand waves in areas with a muddy, silty or clayey fraction, as shown for the North Sea by Baas et al. (2016) and Van Dijk et al. (2012). It is even suggested that clean sands can still contain a mud percentage of 5-10% (Schindler et al., 2015). Also in experimental set-ups on ripple formation (see e.g. Schindler et al., 2015; Wu et al., 2023), ripples are found for relatively small clay cohesive sediment fractions: if the cohesive sediment fraction exceeds roughly 10-15%, bed forms are no longer found (Baas et al., 2016; Schindler et al., 2015). Some authors put this threshold lower, suggesting that even small amounts of cohesive sediment inhibit sand wave formation (Hulscher & Van Den Brink, 2001). Also, silt and sand-sized mud aggregates turn out to allow for the generation of bed forms (Baas et al., 2016). These bedforms are then found to be shorter and lower compared to the bed forms found in non-cohesive sediments (Schindler et al., 2015; Wu et al., 2023).

[1] These exact values might slightly vary depending on the source used. Some authors use a maximal diameter for silts of 62.5 μm.

3.10.3 Modelling

The modelling of sand-mud mixtures is rather involved, as the cohesion will change the erosion properties of the subsoil and also its roughness, compaction properties and nutritional value for benthic organisms (Schindler et al., 2015). Furthermore, the variation of the bonding strength of different types of clay also alters the results obtained (Schindler et al., 2015). An extensive review of different parametrisations for cohesive sediment mixtures is given by Van Rijn (2020); here, parametrisations specifically designated for sand-mud mixtures will be explored. Colina Alonso et al. (2023a, b) showed that including the effect of mud on roughness properties can drastically affect the model outcomes in the setting of an intertidal area. However, these formulations are not further explored in this chapter.

3.10.4 Modelling Bedload Transport

How to model mixtures depends on which type of sediment transport is considered: when bedload transport is considered (e.g Campmans et al., 2017, for a case without mud), the bed evolution is computed as the divergence of the bedload transport. Hence, no explicit consideration needs to be taken of the erosion/deposit equations, and the influence of the mud only influences the parameters of the bedload transport equation. A simple implementation of this is provided by Van Ledden (2001), where the bedload transport can be influenced via the transport parameter T, as $T = (\tau - \tau_{cr})/\tau_{cr}$ where τ_{cr} is allowed to vary as a result of mud content. The formulation would then look like

$$\boldsymbol{q}_b \sim \left(1 - \frac{\mu_m}{\mu_{cr}}\right) T \cdot \mathcal{H}(\mu_{cr} - \mu_m), \quad \text{with} \quad T = \frac{\tau - \tau_{cr}}{\tau_{cr}} \tag{3.19}$$

with μ_m the mud content and μ_{cr} the critical mud content. It can be seen that not only the transport parameter T but also the bedload transport $\boldsymbol{q}_b$ itself is directly influenced by the mud content. However, a variety of different formulations is available, also see Deltares (2023, Chapter 11).

3.10.5 Modelling Suspended Load Transport

Including cohesive sediment in the suspended load formulation is more involved as the cohesive sediment affects different suspended load processes. First, the erosion behaviour of the deposit is influenced due to the cohesion, directly influencing the term E_s in the bottom boundary condition and the bed evolution equation. Secondly, the diffusion of sediment in suspension may depend on the fraction considered. Thirdly, the settling of the suspended sediment may depend on the cohesive sediment concentration, affecting both the settling and the deposition via the settling velocity. Each of these will be discussed separately in the following sections.

Influence on Erosion

Most studies apply a Partheniades erosion equation (see Eqn. 3.13) for sand, mud and mixtures. However, the way the mud content is incorporated differs per study. For instance, Le Hir et al. (2011) choose to distinguish three regimes: if the mud content is below $\mu_{cr,1} = \alpha D_{50} \sim 20 - 40\%$, the sediment is considered as sand and variables $E_0, \tau_{cr,e}, n$ are taken for sand; if the mud content is exceeding $\mu_{cr,2} \sim 70\%$, the sediment is considered as mud and variables are considered for a mud; in between, a linear interpolation of these variables by mud content is used. A similar approach is adopted by Mengual et al. (2017), yet with a lower $\mu_{cr,1} \sim 10 - 20\%$ and applying exponential interpolations rather than linear ones. This is visualised in Figure 3.3, showing various interpolations for these three properties for various values of the lower threshold $\mu_{cr,1}$: 20% (red), 10% (green), 5% (blue) and 0% (yellow). It can clearly be observed that the application of exponential interpolation increases the sensitivity to mud content. Furthermore, this study allows for varying grain sizes as E_0 is taken as a function of the fall velocity and median grain size, following

$$E_0 = \frac{0.015 \rho_s D_{50} w_s}{h_{ref} {D_{50}^*}^{0.3}}, \tag{3.20}$$

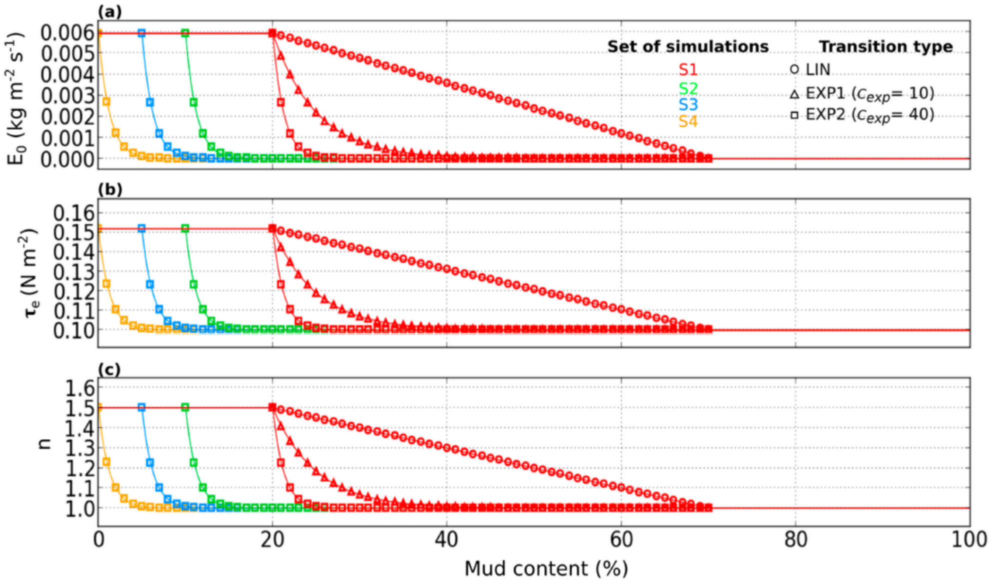

Figure 3.3: Visualisation of the interpolation of the sediment properties E_0, τ_e and n as a function of the mud content. A linear (circles) and two exponential (triangles and squares) interpolation is shown, for various values of $\mu_{cr,1}$ (colours). Courtesy to Mengual et al. (2017).

with ρ_s the density of the sediment, D_{50} the median grain size and D_{50}^* its dimensionless counterpart, and h_{ref} the concentration reference height. An approach similar to this is adopted by Van Ledden (2001).

A slightly different approach is only considering two regimes, a non-cohesive and cohesive one, as done by for instance Colina Alonso et al. (2023a). In the non-cohesive regime ($\mu < \mu_{cr}$), the transport is computed as fully non-cohesive, yet the critical bed shear stress of the non-cohesive fraction is slightly modified for the mud presence following

$$\tau_{cr} = \tau_{cr,s}(1+\mu)^{\beta}, \qquad \beta \approx 0.75 - 1.25 \tag{3.21}$$

with τ_{cr} the critical erosion shear of the mixture and $\tau_{cr,s}$ the critical erosion shear of the non-cohesive fraction in the absence of any mud. This can be used to compute the erosion of the sandy fraction, after which the erosion of the muddy fraction is taken proportional to the erosion of the sandy fraction: $E_m = E_s\mu/(1-\mu)$. It should be noted that this approach yields an influence on the critical erosion shear below the critical mud content as well.

In the cohesive regime, the erosion is computed as

$$E_s = (1-\mu)M_c\left(\frac{\tau}{\tau_{cr,mix}} - 1\right)\mathcal{H}(\tau - \tau_{cr,mix}) \tag{3.22}$$

$$E_m = \mu M_c\left(\frac{\tau}{\tau_{cr,mix}} - 1\right)\mathcal{H}(\tau - \tau_{cr,mix}) \tag{3.23}$$

$$\tag{3.24}$$

where $\tau_{cr,mix}$ (the critical erosion shear of the mixture) and M_c (erodibility of the mixture) are linearly interpolated between μ_{cr} and the full mud case. Equivalently, one can apply the interpolation to the resulting erosion fluxes, which is particularly convenient in the case of multiple sediment fractions (Colina Alonso et al., 2023b).

It should, however, be noted that the lower limits for an influence of the mud content on the erosion properties are still higher than what is generally found in sand wave areas. In the limit of low mud content, the erosion of sand and mud is coupled and hence, the mud content of the bed is not changing due to erosion processes (Colina Alonso et al., 2022). This is also implicit in the models by Le Hir et al. (2011) and Mengual et al. (2017); Van Ledden (2001) applies different expressions for the erosion of both fractions, hence not demanding that the mud content in the bed remains constant under only erosion processes.

Influence on Diffusion

The vertical mixing coefficient ($K_{s,z}$ in Eqn. (3.10)) is sometimes also allowed to be different for mud and sand, as also in Deltares (2023) and Van Ledden (2001). These are determined by

$$K_{s,z} = \begin{cases} 1.4 & \text{for mud,} \\ 1 + 2\left(\frac{w_s}{u^*}\right)^{1.4} & \text{for sand,} \end{cases} \tag{3.25}$$

where u^* is the shear velocity.

Influence on Settling and Deposition

If flocculation does not play a role, the deposition of sand and mud can be treated independently (Colina Alonso et al., 2022), an approach adopted by Van Ledden (2001). However, if this process is important, this has to be considered when evaluating the settling velocity and, consequently, when computing the deposition as D_s depends on w_s. Such an approach is presented by Le Hir et al. (2001), Le Hir et al. (2011), and Mengual et al. (2017), taking an explicit equation describing the settling velocity as a function of the mud content. For sand mixtures, they take the Soulsby formulation, reading

$$w_{s,sand} = \frac{\nu}{D_{50}}\left[\sqrt{10.36^2 + 1.049{D^*_{50}}^3} - 10.36\right], \tag{3.26}$$

with ν the kinematic viscosity. For mud, it is assumed to depend on the concentration and turbulence as a result of flocculation, such that

$$w_{s,mud} = \max\left[w_{s,min}, \min\left[w_{s,max}, k, c_{mud}^m \cdot \left(\frac{1+aG}{1+bG^2}\right)\right]\right],\ G = \sqrt{\frac{\epsilon}{\nu}}. \tag{3.27}$$

Here, the terms k, m, a and b are to be calibrated, whilst $w_{s,min}$ and $w_{s,max}$ (resp. the minimal and maximal fall velocity) are soil properties; furthermore, ϵ is the turbulence dissipation rate. Although this formulation does allow for the correction of the settling velocity based on mud concentration, it has the disadvantage that quite some parameters are to be calibrated or measured; Mengual et al. (2017) gives an estimate for these.

An approach that takes fewer parameters to calibrate is provided by Deltares (2023), amongst various other options (see Sections 11.2.1-11.2.8). This approach takes a similar (though more complicated) expression for the dependency of the settling velocity of the sand fraction on the grain size. For the mud fraction, an easier expression is taken, reading

$$w_{s,mud} = w_{s,mud,0}\left(1 - \frac{c}{c_{stop}}\right)^5, \tag{3.28}$$

with c_{stop} a reference concentration at which settling effectively stops (in the order of 1600 kg m^{-3}). Other corrections for the effect of salinity and temperature are also available but not reviewed here.

3.10.6 Measurements on Critical Shear Stress

The main parameter influenced by the mud content in the previous formulations is the critical shear stress. Hence, some field measurements aimed at finding the critical shear as a function of the mud content are also reviewed. Le Hir et al. (2007) only observes a substantial effect around 40% mud content, a conclusion not shared by other authors. For instance Mitchener et al. (1996) observes a profound effect of the mud content on the critical shear, even for low mud contents. This conclusion is shared by Jacobs et al. (2011) (reporting an increase of the critical shear stress with a factor 1.5 for roughly 10% mud) and Chen et al. (2018), Chen et al. (2021) (reporting a doubling for roughly

10-15% mud). The latter study is particularly interesting as a more general parametrisation for the critical shear stress is presented, also depending on other sediment properties like the median grain size of the sand and mud fraction as well as their densities. In their study, this fit is based on the measurements from multiple previous authors, improving confidence in the fit yet also introducing uncertainty about the exact impact of mud content on erosion properties. With their formula, however, one can obtain these for our case in the North Sea. Furthermore, the fit also shows that consolidation processes are not important for low mud contents up to 15% (Chen et al., 2018; Chen et al., 2021). Fits by other authors are also reviewed by these authors.

The formulation derived by Chen et al. (2021) is relatively straightforward and contains few variables to be determined/calibrated, making it relatively suitable for idealised modelling. For the mud content below the critical mud content (typically 15%), hence for the setting of sand wave fields, the expression reads

$$\tau_{cr} = \theta_{cr0}(d_s^*)(\rho_{ps} - \rho)gd_s + A\frac{1}{d_m}\left(\frac{\rho_{dm}}{\rho_{pm}}\right)^{2/3}\left[\left(\frac{\rho_{dm}}{\rho_{pm}}\right)^{-1/3} - 1\right]^{-2} e^{2.4\frac{\rho_{dm}}{\rho_{pm}}}. \tag{3.29}$$

Here, the fraction ρ_{dm}/ρ_{pm} (the dry bulk density of the mud component in the mixture relative to the density of the mud particles) is controlling the critical erosion shear stress and can be computed following

$$\frac{\rho_{dm}}{\rho_{pm}} = \frac{1}{\rho_{pm}}\frac{\rho_d\mu}{1 - \rho_d/\rho_{ps}(1-\mu)}. \tag{3.30}$$

In these equations is $\theta_{cr0}(d_s^*)$ the critical Shields number of the non-cohesive sediment as a function of the non-dimensional sand grain size, which is computed following the equation by Soulsby; ρ_{ps} the density of the sand particles; ρ_{pm} the density of the mud particles; ρ the density of water; ρ_{dm} the dry bulk density of mud; ρ_d the dry bulk density of the mixture; d_s the diameter of the sand particles; d_m the diameter of the mud particles. The parameter A is to be calibrated, for which Chen et al. (2021, Table 3) provide various estimates for different soils.

The influence of the mud content is not only observed in the critical erosion stress but also the erosion rate, with Mitchener et al. (1996) observing a reduction by a factor 5 if more than 3% mud is added to the sand. This strong dependency is also observed by Perera et al. (2020) and, to some extent, included in the model by Mengual et al. (2017) using an exponential dependency on the mud content.

Chapter 4

Biotic Influences

This chapter discusses the effect of benthic organisms on sand wave dynamids. The chapter starts with a general description of benthic organisms in the North Sea, followed by describing benthos from a modelling perspective and the different mechanisms via which benthic organisms affect their environment. Finally, their influence on sand waves specifically is explored.

4.1 Benthic Organisms in the North Sea

Within the North Sea, a vast variety of different benthic species can be found (see e.g. De Jong et al., 2015), each with their own specific influence on the ecosystem. The occurrence of these species is influenced by, for instance, mud content of the soil, average grain size, bed shear stress, salinity near the bed, amount of organic matter and nutrients in the soil, turbidity of the water and seasonal variation (Baptist et al., 2006; De Jong et al., 2015). Human interventions like dredging also have a pronounced effect (Witbaard & Craeymeersch, 2023), which interestingly can also foster the growth of some species (De Jong et al., 2015); this is further explored in the next chapter.

Importantly, only a few organisms can be classified as "ecosystem engineers": "organisms that directly or indirectly modulate the availability of resources (other than themselves) to other species, by causing physical state changes in biotic or abiotic materials. In so doing they modify, maintain and/or create habitat." (Jones et al., 1994, p. 374) These are also the most relevant species when modelling the hydrodynamics and/or sediment dynamics, as these key species influence their surroundings in such a way that they should be included as functional components of the system (Corenblit et al., 2011). Within the sand wave fields in the North Sea, three species, each modulating their environment in their own distinct way (see Borsje et al., 2009a), are often found (although other species are found as well)

***Echinoidea*,** which are different types of sea urchins, have shown to rework the surface sediment layer. As a deposit feeder, this species may rapidly transport sediment to a deeper layer, promoting a heterogeneous sediment composition. Consequently, the top layer of the sediment may be significantly coarser than a few centimetres deeper for two reasons. Firstly, the organism feeds on organic matter which is generally associated with finer sediment; hence, the organism will move to a new spot once it has reworked all fine sediment, leaving the coarse sediment in the top layer. Secondly, the chance of being ingested and transported to a deeper layer is larger for a smaller particle due to the relatively larger surface area. A comparable organism has shown to be able to double the median grain size in the top layer compared to the case without this organism (Borsje et al., 2009a).

***Terrebellidae*,** which are polychaete worms, may significantly affect near-bed flow due to their tube-building activities. This fosters the settlement of finer sediments. This combined effect may again yield reduced ripple heights within the patches, which reduces the bed roughness (Borsje et al., 2009a).

Bivalves are known to influence the bed erodibility by their burrowing activities (Borsje et al.,

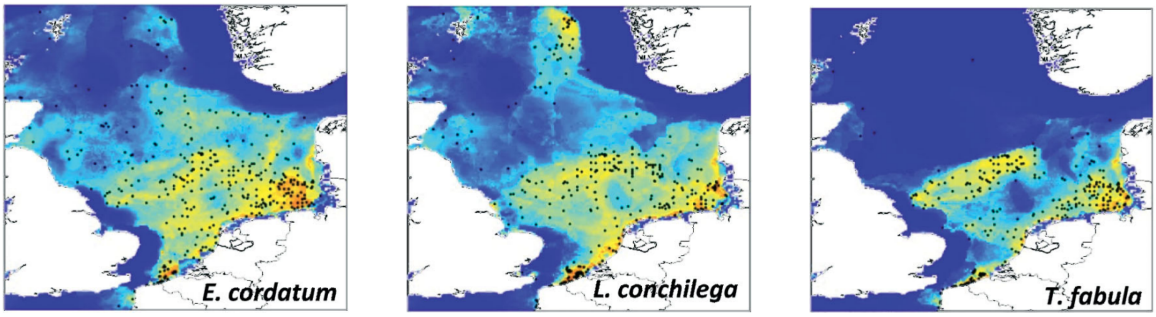

Figure 4.1: Visualisation of the probability of occurrence (color: red = high probability, blue = low probability) of *E. Cordatum*, *L. Conchilega* and *T. Fabula* on the Netherlands Continental Shelf. Black dots denote observed occurrences. Courtesy to Reiss et al. (2011).

2009a). Due to their burrowing and feeding on suspended sediment, the bed erodibility increases, a relation that is quantified by e.g. Borsje et al. (2008). Conversely, shelf fragments may greatly decrease the erodibility of the bed (Cheng et al., 2021a).

Within the sand wave fields, all species are found in the trough region, with the sea urchins and bivalves focussing on the steep slope and the worms on the trough and gentle slope (Cheng et al., 2021a). Additionally, these species are occurring on large parts of the Netherlands Continental Shelf as visualised by Reiss et al. (2011), see Figure 4.1.

On evolutionary timescales, the impact of benthic organisms on their environment should also be perceived from an evolutionary perspective. For the individual organism, being able to slightly more modify the environment to their liking can increase their chances of survival (Corenblit et al., 2011). However, the environmental changes also affect the other organisms, which need to adapt to this as well or can even extinct (Jones et al., 1994). Some authors even claim that ecosystem engineering has been vital for making the Earth suitable for the currently existing forms of life (Meysman et al., 2006).

4.2 Benthic Organisms from a Modelling Perspective

As already indicated, incorporating the ecosystem engineers in a model is most relevant from a modelling point of view, as these species have the largest effect on the system behaviour (Corenblit et al., 2011). It is postulated that all ecosystems are controlled by only a small set of key species (Widdows & Brinsley, 2002). Importantly, such a modelling practice does not only involve feedbacks describing how the organisms control their environment but also how the growth and decay of organisms are affected by the environment (Corenblit et al., 2011). The effect of organisms on their environment will be further explored in the sections to come, here we will focus on controls on benthic growth.

Different interactions between the benthic organisms and their environment can be included to model their influence. Currently, modelling studies in the field of sand wave dynamics that included benthic organisms only take bed shear stress as a control on benthic growth: the larger the shear stress at a given location, the lower the carrying capacity at that location (Damveld et al., 2020b; Damveld et al., 2019). The growth and dispersal of the organisms themselves are also included, but any other possible controls from the system are omitted. This shortcoming is also recognized by Damveld et al. (2020b), suggesting the use of sediment type and size as a predictor for the occurrence of polychaete worms. In the context of intertidal salt marsh development, Van De Koppel et al. (2001) also suggests incorporating a dependency on the silt content of the soil, commonly used as a proxy for nutrient presence in the soil. This mathematical formulation would then take the form

$$\frac{dS}{dt} = \text{deposition}(\tau) - \text{erosion}(\tau, S, D), \tag{4.1}$$

$$\frac{dD}{dt} = \text{growth}(S, D) - \text{decay}(\tau, S, D), \tag{4.2}$$

with S the silt content, τ the bottom shear stress and D the benthic organism population. Constraints on the shape of the different functions are also given, for which we refer to Van De Koppel et al. (2001, Table 1). Fieldwork by Kooistra et al. (2023) confirms that different species prefer different types of sediment, and also that species have different tolerances to deviations from their preferred grain size: at the ends of the spectrum, species can be "sensitive specialists" or "tolerant generalists" (Kooistra et al., 2023). Other feedbacks can also be included, for instance, the control of the suspended sediment concentration on the benthic growth rate due to turbidity processes (Le Hir et al., 2007).

Importantly, there must be a balance between the physical and ecological control of the system: if this is the case, the two can co-evolve together to a system in which both control the environment to some extent. In case this balance is absent, however, the system can be dominated by either the physical forcing (e.g. strong currents flushing away the vegetation in a salt marsh) or the organisms (e.g. dense vegetation impeding any sediment dynamics). Only in a balanced system, the two can interact and both exert some control on the system development (Corenblit et al., 2011).

4.3 Organism-Morphodynamics Interactions

4.3.1 Introduction

Benthic organisms can be organised by their micro-scale influence on the system, for instance by increasing bottom drag or grain sorting. The next subsections explain a different mechanism via which the benthic organisms can influence the hydrodynamics, sediment dynamics or bed behaviour.

However, we can also classify the organisms by their macro-scale influence on the bed. This leads to two distinct classes: species that stabilise and destabilise the bed. Stabilisation can be the result of a reduction of the current velocity, reduction of wave action or enhancement of sedimentation or cohesive properties of the sediment (Widdows & Brinsley, 2002). This can be caused by physically covering the sediment (e.g. mussel beds), sediment binding by roots (e.g. salt marsh vegetation) or organisms excreting extracellular polymeric substances (Paarlberg et al., 2005; Widdows & Brinsley, 2002). Borsje et al. (2009b) classifies the polychaete worms and sea urchins as stabilisers, although this does not necessarily inhibit sand wave formation as shown by Damveld et al. (2020b). Destabilisation of the bed is caused by for instance increased porosity, deposit-feeding or increased mixing (Paarlberg et al., 2005). Such organisms increase the sediment transport compared to the case without organisms, which is for instance done by bivalve shells (Borsje et al., 2009b; Widdows & Brinsley, 2002).

4.3.2 Organisms Influencing Near-Bed Flow

Benthic organisms may form a major control on the bed roughness (Baptist et al., 2009; Borsje et al., 2009a). This change in roughness can, for example, be caused by shells or shell fragments: an increased presence of these yields a smoother surface and lower ripples, hence increased flow velocities near the bed (Cheng et al., 2021a). Vegetation and algae can also fulfil this function, as it has been shown that the presence of the algae species *Enteromorpha* can reduce the current speed by 15% to 42% (for resp. 10% to 60% of the surface covered by algae; Widdows & Brinsley, 2002). Finally, bottom structures created by organisms can induce larger bed roughness (Murray et al., 2002).

In sand wave fields, the polychaete worm *Lanice conchilega* is often observed, a species that builds small tubes protruding out of the bed. Locally, this species can have a density of up to 3000 individuals per square metre (Borsje et al., 2009a), although there seems to be a large variability in

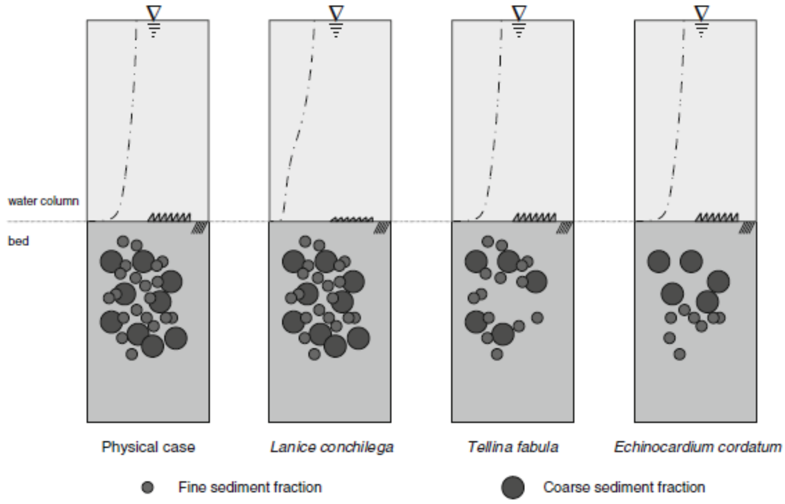

Figure 4.2: Influences of three different benthic species on near bed flow, sediment sorting and bed roughness. Courtesy to Borsje et al. (2009b).

the densities. For a small density of tubes, these lead to increased erosion due to flow concentration around the tubes (scour); for larger densities (already starting at 500 ind. m^{-2}), the increased drag slows down the flow or even skimming can occur when the flow goes over the tubes instead of through them, protecting the bed against erosion (Baptist et al., 2009; Murray et al., 2002). It is, therefore, no surprise that the density of the patch *Lanice conchilega* is a major control on the morphodynamics, much more than the tube height (Borsje et al., 2009b). Patches of *Lanice conchilega* slow down the near-bed flow up to 30%, fostering the deposition of fine sediments and yielding a decrease in ripple height of up to 80% (Borsje et al., 2009a; Borsje et al., 2009b). As a consequence of this, the near-bed eddy viscosity is lower, thus yielding decreased sediment transport rates and thus shorter wave-length features (Borsje et al., 2009a). Additionally, the tubes form a shelter for other organisms (Borsje et al., 2009b; Damveld et al., 2020b).

The effect of *Lanice conchilega* has been successfully implemented in sand wave models, see for instance Borsje et al. (2009a), Damveld et al. (2019) and Damveld et al. (2020b). The effect on the bottom friction is included in two different ways: in Damveld et al. (2020a) and Damveld et al. (2019), the presence of organisms increases the slip-parameter in their idealised model, whilst Borsje et al. (2009b) include the biotic influence on the ripple height, hence yielding an indirect influence of the *Lanice* on the bed roughness (also see Figure 4.2).

4.3.3 Organisms Influencing Bed Erodibility

The erodibility of the sediment, which is defined as “the capacity of a sediment to be eroded when submitted to a hydrodynamic forcing” (Le Hir et al., 2007, p. 1117), is strongly depending on the cohesion of the upper sediment layer. As this can have a large influence on the sediment transport, also the large-scale morphodynamics can be influenced by local changes in the bed erodibility (Le Hir et al., 2007; Le Hir et al., 2005). The erodibility can be reduced in different ways, for example by chemical bonding of the sediment grains by extracellular polymeric material, physical coverage of the bed by shells or algae and retaining of the soil by for instance roots of plants (Baptist et al., 2009; Murray et al., 2002). As mentioned before, the presence of algae can significantly reduce sediment erosion (Widdows & Brinsley, 2002). However, also shells can have a large influence, as Cheng et al. (2021a) showed that only 2.5% (in volume) shell content already tripled the critical erosion shear stress. Interestingly, larger percentages of shell content made the critical bed shear stress decrease again (to 25% higher than the default case for 15% shells), to afterwards increase again to 2.5 times the default value for 50% shell content (Cheng et al., 2021a).

Erosion can also fostered by organisms, for instance due to burrowing activities that disturb

(a) *Lanice Conchilega*,
courtesy to www.waarneming.be.

(b) *Echinocardium Cordatum*,
courtesy to Damveld et al. (2019).

Figure 4.3: Examples of benthic species: a species influencing near-bed flow (*Lanice conchilega*; left panel) and influencing sediment sorting (*Echinocardium cordatum*; right panel).

the top layer of the soil (Borsje et al., 2009a). Examples of these are the bivalve species *Mahoma baltica* and *Fabulina fabula*, typically occurring with around 25 individuals m^{-2} (Borsje et al., 2009a). Both species are known to disturb the bed (Widdows & Brinsley, 2002), and the relation between the presence of *Mahoma baltica* and critical shear stress is explicitly known (see Le Hir et al., 2007). Both the relation by Le Hir et al. (2007) and the modelling work by Borsje et al. (2009a) show that very low densities of either of the bivalves already greatly reduce the critical bed shear stress, hence increasing the bed and suspended load transport depending on the exact flow conditions (see Fig. 4.2). In particular, if the default shear stress is just below the critical shear stress, the addition of bivalves to the system can allow for sediment transport to occur, hence having a large influence on the observed bed features (Borsje et al., 2009a).

4.3.4 Organisms Sorting Grain Sizes

Burrowing organisms are known to change the grain size in the top layer of the soil, consequently changing the erosion and friction properties of the bed (Baptist et al., 2009). As a consequence of digging, deposit-feeding or movement through the sediment, loosening of the soil can occur which makes the soil more susceptible to erosion (Meysman et al., 2006; Murray et al., 2002). Additionally, deposit-feeding can bring finer sediments to the surface of the soil, which are easily eroded. If no other organisms are present that mix the soil, this can eventually yield erosion of the soil and the formation of coarse-grained areas (Murray et al., 2002). The reduction of mud content furthermore affects other organisms living at that location or the erosion properties as the sediment can turn to non-cohesive (Paarlberg et al., 2005). Finally, grain sorting can also influence the elastic properties of the sediment, which in turn may influence the wave attenuation properties (Murray et al., 2002).

One of the deposit-feeding species is *Echinocardium cordatum*, typically occurring with 15 individuals m^{-2}, transporting the finer sediments deeper into the soil (Borsje et al., 2009a). This results in coarsening of the bed, which yields longer wavelengths of the bottom features due to reduced sediment transport by suspended and bedload transport (Borsje et al., 2009a). In a modelling study by Borsje et al. (2009b), this species was incorporated by using two soil layers: an active top layer and a passive bottom layer. As the top layer thickness equalled the region of influence of *Echinocardium cordatum*, the effect of the benthic organisms was incorporated by changing the average grain size of the top layer (Borsje et al., 2009b, Fig. 4.2).

4.3.5 Organisms Influencing Slope Failure

Some benthic organisms are also known to stabilise slopes by increasing the angle at which slope failure occurs (Baptist et al., 2009). Different mechanisms are possible to achieve this, for example, pile reinforcement of the slope, cementation of the grains or the coverage by microalgae (Murray et al., 2002). Another mechanism is that sediment sorting organisms can prevent the formation of potential failure planes as a result of their activities (Murray et al., 2002). As the failure angle of the soil can be increased by up to 15 degrees for fine-grained sand (Le Hir et al., 2007), these organisms could have a drastic effect on bottom features. Also in the context of salt marshes, the slope stabilisation is observed (Paarlberg et al., 2005).

4.3.6 Biodeposition

Some benthic organisms induce additional fluxes of fine sediment from the sediment to the water column (deposit feeders ejecting faeces) or from the water column to the sediment (bio-deposition induced by suspension feeders; Le Hir et al., 2007). This can result in a significant amount of deposition, for instance done by bivalves (Murray et al., 2002), mussels and some algae species (Widdows & Brinsley, 2002). These species influence the dynamics in different ways: they reduce the suspended sediment load, change the composition of the top layer of the bed and can increase the bottom roughness due to the creation of biogenic mounds. In the model of Damveld et al. (2019), this latter effect is incorporated by changing the slip parameter. It should, however, be noted that the biogenic mounds are three-dimensional features, being roughly as wide as they are long. Consequently, the flow is not necessarily diverted over them, but potentially also around them (Damveld et al., 2020b). The study by Borsje et al. (2014) showed that the flow around the patches is roughly 10 times smaller than the flow over the patch allowing for a 2DV approach, yet such an approach introduces an important uncertainty to consider when interpreting the result (Damveld et al., 2020b).

4.3.7 Organisms Compacting Sediment

Digging organisms can compact the sediment in a direction perpendicular to the direction of digging. This reduces the voids in the material and increases the critical bed shear stress of the soil, which can, in turn, affect the larger-scale bedforms. At low densities, only local strengthening occurs, potentially leading to patchy erosion. For larger densities, this would yield larger areas that are prone to less erosion (Murray et al., 2002).

4.3.8 Biological Armouring

Different organisms can induce bottom armouring, either directly or indirectly. Larger organisms like shells and mussels can armour the bed by physically protecting it from erosion, something that can be further increased by thread networks produced by some of these organisms (Murray et al., 2002). As a consequence of their protection and effect on the friction drag, the stability of the bed can be increased significantly (Widdows & Brinsley, 2002). In the case of shells, (Cheng et al., 2021a) showed that an increasing shell content can yield immobile shell clusters that armour the bed. In the context of ripples, Cheng et al. (2021b) showed that shell fragments can already function as armouring.

Armouring can also occur indirectly through the effect of winnowing. If the bed shear stress is strong enough to erode fines, but too weak to erode coarser fractions, the bed coarsens and is armoured by the coarse sediment layer (Cheng et al., 2021a). This process can also be moderated and accelerated by organisms, for instance species bringing fines to the surface (see Sec. 4.3.4).

Main paper: Murray et al. (2002)

4.3.9 Organisms Excreting Extracellular Polymeric Material

The effect of organisms excreting extracellular polymeric materials has already briefly been touched on in Section 4.3.3, as one of the effects of this material is that grains stick together. Consequently, the material is more difficult to erode and can have a higher failure angle (Murray et al., 2002; Widdows & Brinsley, 2002). However, this material has a few more influences on the system: it can cause increased sedimentation rates as a consequence of flocculation; it can reduce the effect of drag by suppressing turbulence near the bed due to increasing the viscosity of the fluid; and it can

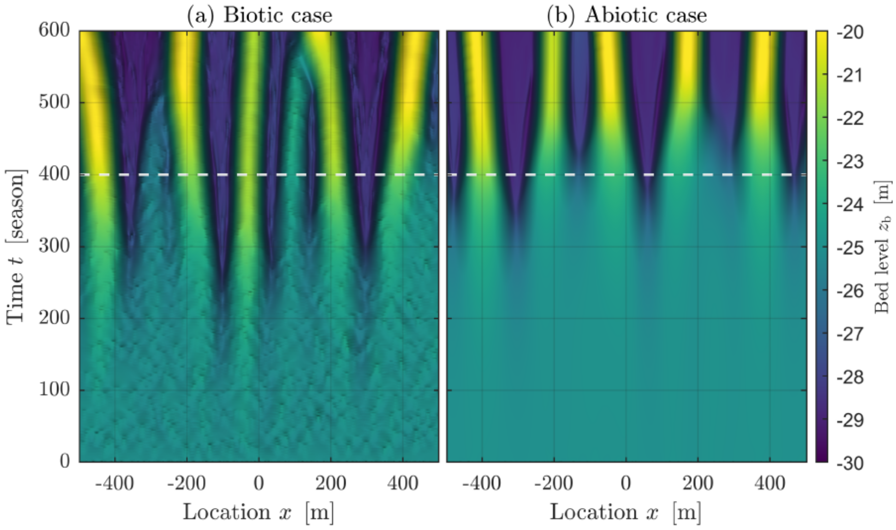

Figure 4.4: Visualisation of how the presence of *Lanice conchilega* may influence the development of sand wave fields, contrasting the case without (left panel) and with (right panel) these organisms. Courtesy to Damveld et al. (2020b).

block pores, yielding higher permeability of the soil and thus altered erosion properties and altered settlement properties for other organisms (Murray et al., 2002).

4.4 Biota Influencing Sand Wave Dynamics

Both field measurements and modelling studies show that the presence of benthic species can have a significant effect on the dynamics of sand waves (see e.g. Damveld, 2020). The field study by Baptist et al. (2006) reports significant seasonal variability in the benthic assemblages, except for assemblages in sand wave troughs. Also field observations from Cheng et al. (2021a) and Damveld et al. (2018) report higher concentrations of species at the trough and steep slope, up to a factor 30 higher compared to the crest (Damveld et al., 2018). This is confirmed by the modelling study by Damveld et al. (2019), also showing that the presence of a residual current can cause the highest animal densities to be located at the steep slope rather than in the trough. Fieldwork by Van Dijk et al. (2012) also reports increased animal densities in the troughs, suggesting that this is caused by the accumulation of fine sediments in the trough, making it a more favourable place for biota to settle. In a similar vein, dead organic matter and nutrients could accumulate here, which, combined with the sheltering effect, could lead to a local bloom of benthic organisms (Damveld et al., 2018).

Modelling studies also show that the presence of biota can result in the formation of bedforms when a flat bed is anticipated, or maintain a flat bed whilst the physical forcing allows for bed forms to develop (Borsje et al., 2009a). As such, benthic organisms can yield the growth of sand waves, but sand waves can also yield the formation of benthic patches (Damveld et al., 2019). If these organisms are present, it has been shown by Damveld et al. (2020b) in a modelling study that the sand wave height can be affected in the order of decimeters, like the wavelength and the time it takes to converge to the equilibrium. It is also shown that the wavelength of the fastest-growing mode can shift over time under the influence of the presence of benthic species (Damveld et al., 2020b). The influence of these organisms on the bed in the initial formation phase is illustrated in Figure 4.4; for visualisations of the effect of this species on sand wave characteristics, the reader is referred to Damveld et al. (2020b).

Chapter 5

Marine Sand Extraction

In this chapter, the relevance of investigating sand extraction is discussed. We first discuss the sand extraction policy on the Netherlands Continental Shelf (how much sand is extracted and anticipated to be extracted, and what are the most relevant policies surrounding this), after which the influence of sand extraction on the sea bed, sediment properties and biota is discussed using field observations and modelling work. The relevance of a coherent strategy for sand extraction is underpinned by UNEP (2022), recommending qualifying sand as a strategic resource to avoid uncontrolled exploitation of this resource. Currently, sand is one of the world's most-extracted minerals (Schandl et al., 2016), and the currently observed growth in sand extraction rates is not expected to decrease.

5.1 Sand Extraction on the NCS

The amount of sediment, extracted from the Netherlands Continental Shelf, is expected to increase at least twofold in the upcoming decades due to climate change. In the current situation, 13 million m^3/yr is extracted as filler sand, whilst roughly 12 million m^3/yr is extracted to maintain the coastline and enable growth with sea level rise (Haasnoot et al., 2018). However, this latter amount anticipated to increase depending on the rate of sea level rise (Ministerie van Infrastructuur en Waterstaat et al., 2022), where the Deltacommissie (2008) estimates that 7 million m^3/yr is required for each millimetre of sea level rise per year. This yields an estimate of 40 to 85 million m^3/yr (Deltacommissie, 2008), but this could increase to 240 million m^3/yr in the worst sea level rise scenario (Haasnoot et al., 2018). Although there is a large difference in the exact estimates, a large increase in extraction volumes seems unavoidable.

These volumes are in principle available on the Netherlands Continental Shelf (see Figure 5.1 for the distribution of sand extraction locations), but due to increasing usage of space for other purposes (e.g. fisheries, nature reserves or wind farms), integrated planning of the sand reserves was required (Deltacommissie, 2008). This should also consider the efficiency and cost-effectiveness of sand extraction, as extracting sand far from the envisioned use location comes with large transportation costs. This puts particular pressure on the Southern part of the Netherlands Continental Shelf, where a need large need for sand is combined with present or planned wind farms and electricity cables (Ministerie van Infrastructuur en Milieu & Ministerie van Economische Zaken, 2014).

For this reason, a new sand mining strategy has been formulated, aiming at better planning of the extraction areas and focusing on deeper extraction (IDON, 2011). Until roughly 2010, shallow extraction was the default, with a maximum depth of two metres. However, the new strategy aims for deeper (over two meters) extraction to increase the amount of available sand and make more efficient use of available sand and space (IDON, 2011; Ministerie van Verkeer en Waterstaat et al., 2009; Staatscourant, 2010). More recent policy explicitly allows even deeper extraction: up to one meter above shallow clay or peat layers to avoid suspension of these sediments (Ministerie van Infrastructuur en Milieu & Ministerie van Economische Zaken, 2014). With this policy, the government also aims to reduce the disturbance of the sea bed, as a deeper excavation allows for less area to be disturbed (Ministerie van Infrastructuur en Milieu & Ministerie van Economische Zaken,

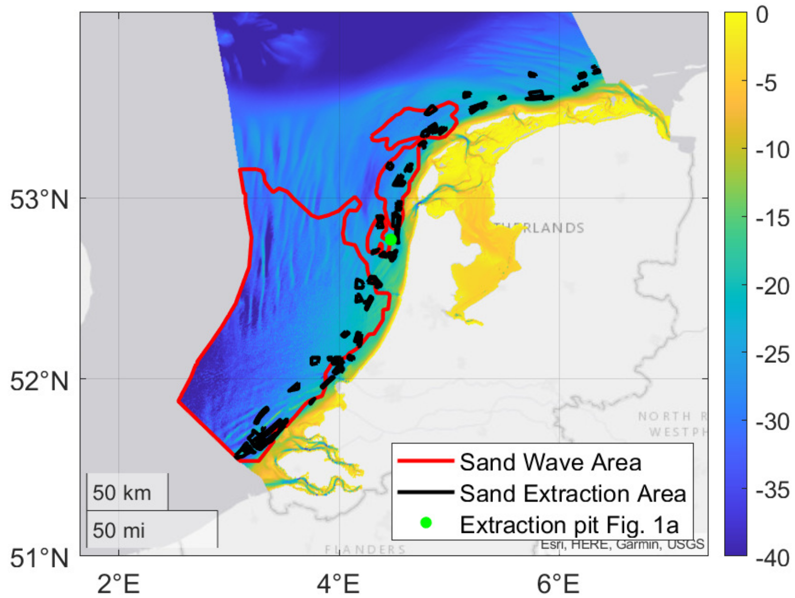

Figure 5.1: Visualisation of the extraction locations on the Netherlands Continental Shelf, combined with the locations of sand waves.

2014; Ministerie van Verkeer en Waterstaat et al., 2009). In line with this policy, extraction pits had an average depth of eight meters depth during the past decade and up to 20 meters depth for specific projects like Maasvlakte 2 (Ministerie van Infrastructuur en Waterstaat et al., 2022).

Extracting sediment is, however, not allowed without a permit (Staatscourant, 2010), which needs to be supplemented with an environmental impact assessment ("Milieueffectrapportage", MER) in case of extracting more than 10 million m^3 or over a surface exceeding than 500 hectares (Ministerie van Infrastructuur en Milieu & Ministerie van Economische Zaken, 2014). For the extraction for sand nourishments, which in total amount to more than 10 million m^3, Rijkswaterstaat has requested one MER based on which the permit has been issued for the period 2018-2027 (Rijkswaterstaat, 2020); the MER is also publicly available, see Sweco (2017).

5.2 Development of Sand Extraction Pits

Execution of a sand extraction forms a significant perturbation of the sea bed, after which the sea bed can either return to the original state or new bedforms like sand waves can be generated. In this section, we only explore the first option.

In general, the evolution of extraction pits after extraction takes two steps. First, the steep slopes at the edges are observed to quickly (within a few months) smoothen out as a result of slope failure and slope-driven sediment transport, initiating backfilling of the deepest areas of the pit (Mielck et al., 2019). This is also observed in the modelling study by Blondeaux and Vittori (2005a). Secondly, the much slower phase of backfilling takes place: for shallower pits, this can be within a decade, but deeper pits remain clearly recognizable in the bed after multiple decades (Mielck et al., 2019; Witbaard & Craeymeersch, 2023). This is also illustrated in Figure 5.2, showing that an extraction pit is still clearly visible in the bed 7 years after the extraction took place. In general, backfilling of the pit is observed, with Mielck et al. (2019) observing backfilling in the order of ten meters over multiple decades, which is explained by the settling of suspended sediment due to a reduction of the flow velocity. Consequently, a pit that is sheltered from storms and winds recovers slower due to the lower amount of suspended sediment (González et al., 2010). This also means that relatively much fine sediment is found in recovering sand pits, with the median grain size decreasing and the mud content increasing Mielck et al. (2019); this is, however, further discussed in Section 5.4.

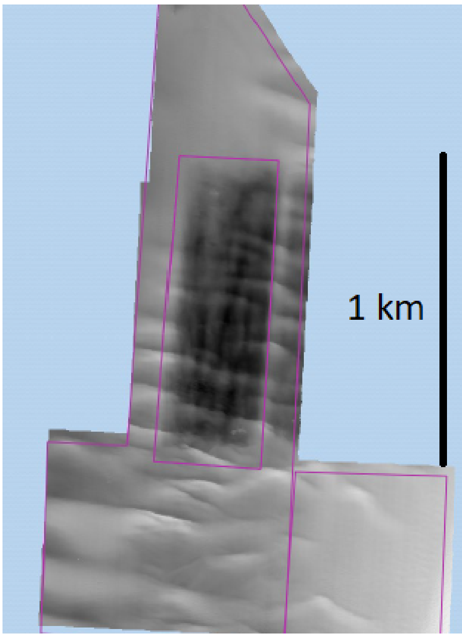

Figure 5.2: Bottom topography of a sand extraction pit 7 years after the extraction took place. Courtesy to Witbaard and Craeymeersch (2023).

González et al. (2010) provide some practical design recommendations to reduce the regeneration time of sand pits, with the general recommendation to have the longest axes normal to the dominant flow direction. In the case of bedload transport dominance, the authors recommend a narrow, deep and long pit. In case that suspended flow is dominant as a consequence of increased wave action, the authors argue there is a balance between infilling due to wave action (increasing recovery) and an increase in migration velocity due to wave action (decreasing recovery) which determines the optimal design (González et al., 2010).

Furthermore, it should be noted that sand pits can also migrate in case a residual current is present, a phenomenon that is explained similarly to the migration of sand waves (Blondeaux & Vittori, 2005a). Also, deformation of the sand pit geometry can take place under the influence of Coriolis effects, causing the pit to take an S-shape and modifying how humps are formed adjacent to the extraction pit (Roos et al., 2008).

5.3 Influence on Sand Waves

Based on field observations, the question arises whether sand waves in a sand extraction pit will always recover. Both De Jong et al. (2014) and Krabbendam et al. (2022) argue that sand waves do not always recover. Krabbendam et al. (2022) motivates that the lacking recovery of sand waves can potentially be caused by changes in sediment size, or that the depth of the extraction pit can play a role as a deeper pit results in lower bottom shear stresses and lower wind and wave action, hence lower sediment mobilisation. Another possibility is the local lack of sediment (Krabbendam et al., 2022). At the same time, examples are also known where sand waves did recover within sand pits: eight years after the extraction, sand pit Q5JP at the Netherlands Continental Shelf is again partially filled in (Witbaard & Craeymeersch, 2023, see Figure 5.2), and also Krabbendam et al. (2022) does observe recovery at one of the surveyed pits. This is particularly relevant as a large amount of the planned sand extraction pits are located within (or close to) the sand wave area on the NCS (see Figure 5.1).

Modelling studies about the specific influence of sand extraction on sand waves are very limited, mainly focussing on dredging instead of extraction. For dredging, Campmans et al. (2021) concludes that with an increasing dredging volume, the recovery time also increases; however, the system itself can come in dynamic equilibrium with the intervention. Furthermore, this study also highlights the importance of sand wave shape and sand waves neighbouring the intervention in the recovery process. In the context of sand waves, Blondeaux and Vittori (2005a) and Roos et al. (2005) concludes that an intervention can trigger the formation of sand waves on a previously flat bed; this is also concluded by Nnafie et al. (2020) in the context of tidal sand ridges, and by Roos and Hulscher (2002, 2003) and Roos et al. (2008) for sand banks.

A few conclusions from the work by Nnafie et al. (2020) are particularly interesting (although in the context of sand ridges): first of all, it concludes that recovery of these features can take in the order of decades and that this time span is reasonably estimated by the estimator introduced in Roos et al. (2008) for sand banks. Secondly, it suggests that reduced wave action increases the recovery time, as also observed by González et al. (2010), a finding particularly important when considering the processes to be included in a model for sand pit regeneration. Thirdly, it suggests that the recovery time might not be proportional to the extraction depth, as a pit with four times the depth was observed to only take ten years longer than the default pit design.

5.4 Influence on Sediment Properties

When it comes to the influence of sand pits on sediment properties, all studies on the Netherlands Continental Shelf observe the same trend: a deep sand extraction pit accumulates fine sediment. This leads to a decreased median grain size and an increased mud content in the pit with up to a factor four (De Jong et al., 2015; De Jong et al., 2014; Hendriks et al., 2020; Mielck et al., 2019; Witbaard & Craeymeersch, 2023). This is explained as a consequence of the settling of fine sediments due to the decreased flow velocities in the pit; this also implies that the sediment is transported not much further than the rim (Mielck et al., 2019). The infilling with large quantities of fine sediment also implies that the sediment should originate from elsewhere in the North Sea, as the vicinity of the pit only contains low amounts of mud (order of 2.5%) whilst the mud content within the pit can increase to 30% (Mielck et al., 2019). Furthermore, this is not the type of sediment that is compatible with the beach environment (Mielck et al., 2019); hence, in the case of extraction for sand nourishments, one can argue whether this is recovery or not. Furthermore, the percentage of organic matter in the soil is also found to increase with the increased mud content (Witbaard & Craeymeersch, 2023).

Interestingly, Witbaard and Craeymeersch (2023) observes a difference in behaviour depending on the depth of the sand extraction pits: for middle deep (four to six meters) and deep sand extraction pits, accumulation of mud and fines was generally observed, whereas this has not been reported for shallow pits. This leads these authors to the suggestion that “already with middle deep extraction, a critical depth is exceeded, [...] [which] could indicate a fundamental difference between the two methods of sand extraction.” (Witbaard & Craeymeersch, 2023, p. 36, translated from Dutch)

5.5 Influence on Biota

The influence of sand extraction on the biota in and around the extraction location can be profound. On the short-term, the benthic organisms are damaged or removed. However, after multiple years, different authors report a drastic increase in the presence of benthic species, ranging from fivefold (de Jong et al., 2015) to sevenfold (de Jong et al., 2016). Also Witbaard and Craeymeersch (2023) notes a large difference. At the same time, de Jong et al. (2015) also reports a decrease in species richness and also de Jong et al. (2016) reports a change in the dominant species, which is sometimes even observed for relatively small changes in the mud content (Witbaard & Craeymeersch, 2023). However, an important caution should be placed by these observations: these were all made for pits which were accreting with cohesive sediments; for pits in areas with more gravel present, this might be vastly different. Witbaard and Craeymeersch (2023) also suggests the importance of local flow conditions and sediment properties in determining how the biota in the pit will develop. Furthermore, the change in benthic species will also induce a change higher higher-order biota, as fish assemblages are also reported to change after the occurrence of a sand extraction, potentially a consequence of the change in benthic species (De Jong et al., 2014).

An interesting observation is made by De Jong et al. (2014) and de Jong et al. (2015), where a sand pit is studied in which an artificial sand bar was left. The authors found that this ecosystem-based landscaping technique significantly influenced the fish assemblages (De Jong et al., 2014) and benthic species densities (de Jong et al., 2015), showing that the application of an ecosystem-based extraction methodology can be used to influence the environmental impact of sand extraction.

Chapter 6

Conclusion

In this chapter, we briefly formulate the answers to the literature questions based on the presented review.

How do different hydrodynamical processes explain and change sand wave dynamics?

Sand wave formation is fully explained by the balance between upward sediment transport (due to a tide-averaged residual flow cell) and downward sediment transport (due to the slope). Sand waves form in case the former dominates, whilst they damp out when the latter dominates. The residual flow cells form due to the interaction of the (wavy) bed with the tidal forcing, causing near-bed flow (and thus sediment transport) towards the crest. The advection of momentum is key to ensure proper alignment of the flow cells and thus allow sand wave growth. The other processes reviewed (Coriolis effect, forced residual flow or higher order tidal constituents) all change this process but do not cause significant changes in the sand wave dynamics. However, residual currents are key to explaining sand wave migration.

How do sedimentological processes and sediment properties interact with sand wave dynamics?

Sand waves only occur in areas where bedload transport is dominant and where the sediment consists mainly of sand. Bedload transport is responsible for the uphill transport of sediment. It is the key process to explain the bed evolution, together with the (downhill) slope-induced transport. However, the contribution of suspended sediment transport (which may be up to 30% of the bedload transport) can still be significant. This contribution is generally dampening sand wave growth, although some authors report increased growth rates depending on the wavelength. The effect of sediment properties and composition can also be profound, in particular the presence of cohesive sediments. Due to its cohesive properties, it will influence the sediment properties of the entire mixture, hence also influencing the properties of the non-cohesive sediment in the mixture.

Which mechanisms govern the interaction between benthic organisms and sand wave dynamics?

Ecosystem engineers are the key organisms to consider when studying the interaction between benthos and their environments. For the Netherlands Continental Shelf, these are *Echinoidea*, a species changing the top layer sediment compositions, *Terrebellidae*, a species changing near bed flow, and bivalves, a species changing bed erodibility. Other species play a smaller role and may have a different influence on the system, for instance by compacting the soil or inducing slope failure. The key influence of the environment on these organisms is typically the bed shear stress, which to a large extent determines whether a location is suitable as a habitat for the organism. In sand wave fields, this causes the benthos to be predominantly located in the troughs of the sand waves, which are sheltered from the currents and generally accumulate fine sediment. In turn, modelling studies suggest that benthos may influence sand wave dynamics in a multitude of ways, showing how they engineer their environment in their favour.

How does sand extraction on the Netherlands Continental Shelf influence the bed morphology, composition and benthic organisms?

Due to the large sand demand and the policy of deep extraction, the impact of sand extraction on the Netherlands Continental Shelf may be profound. Deep extraction pits only recover on a decadal timescale, forming a significant disturbance of benthic life. Furthermore, sand extraction may initiate sand wave formation where these were previously not found, or prevent sand wave formation in places where they were found. This is particularly relevant to the Netherlands Continental Shelf as many planned extraction sites are close to or in sand wave fields. Additionally, sediment properties may change significantly because extraction pits generally accumulate fine sediment. This yields decreased median grain sizes and up to a factor of four increase in the mud content.

Bibliography

Amoudry, L. O., & Souza, A. J. (2011). Deterministic coastal morphological and sediment transport modeling: A review and discussion. *Reviews of Geophysics*, *49*(2), 1–21. https://doi.org/10.1029/2010RG000341

Baas, J. H., Best, J. L., & Peakall, J. (2016). Predicting bedforms and primary current stratification in cohesive mixtures of mud and sand. *Journal of the Geological Society*, *173*(1), 12–45. https://doi.org/10.1144/jgs2015-024

Bacik, K. A., Lovett, S., Caulfield, C. C. P., & Vriend, N. M. (2020). Wake Induced Long Range Repulsion of Aqueous Dunes. *Physical Review Letters*, *124*(5), 054501, 1–6. https://doi.org/10.1103/PhysRevLett.124.054501

Baptist, M. J., Tamis, J. E., Borsje, B. W., & Van Der Werf, J. J. (2009). *Review of the geomorphological, benthic ecological and biogeomorphological effects of nourishments on the shoreface and surf zone of the Dutch coast* (tech. rep.). Wageningen IMARES report C113/08, Deltares report Z4582.50.

Baptist, M. J., van Dalfsen, J., Weber, A., Passchier, S., & van Heteren, S. (2006). The distribution of macrozoobenthos in the southern North Sea in relation to meso-scale bedforms. *Estuarine, Coastal and Shelf Science*, *68*(3-4), 538–546. https://doi.org/10.1016/j.ecss.2006.02.023

Besio, G., Blondeaux, P., Brocchini, M., Hulscher, S. J. M. H., Idier, D., Knaapen, M. A. F., Németh, A. A., Roos, P. C., & Vittori, G. (2008). The morphodynamics of tidal sand waves: A model overview. *Coastal Engineering*, *55*(7-8), 657–670. https://doi.org/10.1016/j.coastaleng.2007.11.004

Besio, G., Blondeaux, P., & Frisina, P. (2003). A note on tidally generated sand waves. *Journal of Fluid Mechanics*, *485*, 171–190. https://doi.org/10.1017/S0022112003004415

Besio, G., Blondeaux, P., & Vittori, G. (2006). On the formation of sand waves and sand banks. *Journal of Fluid Mechanics*, *557*, 1–27. https://doi.org/10.1017/S0022112006009256

Besio, G., Blondeaux, P., Brocchini, M., & Vittori, G. (2004). On the modeling of sand wave migration. *Journal of Geophysical Research: Oceans*, *109*(4), C04018, 1–13. https://doi.org/10.1029/2002JC001622

Blondeaux, P., & Vittori, G. (2005a). Flow and sediment transport induced by tide propagation: 1. The flat bottom case. *Journal of Geophysical Research: Oceans*, *110*(7), 1–13. https://doi.org/10.1029/2004JC002532

Blondeaux, P., & Vittori, G. (2005b). Flow and sediment transport induced by tide propagation: 2. The wavy bottom case. *Journal of Geophysical Research: Oceans*, *110*(8), 1–11. https://doi.org/10.1029/2004JC002545

Blondeaux, P. (2001). Mechanics of Coastal Forms. *Annual Review of Fluid Mechanics*, *33*, 339–370.

Blondeaux, P. (2012). Sediment mixtures, coastal bedforms and grain sorting phenomena: An overview of the theoretical analyses. *Advances in Water Resources*, *48*, 113–124. https://doi.org/10.1016/j.advwatres.2012.02.004

Blondeaux, P., Brocchini, M., Vittori, G., Blondeaux, P., Brocchini, M., Drago, M., Iovenitti, L., & Vittori, G. (1999). Sand waves formation: Preliminary comparison between theoretical predictions and field data. *1st IAHR Symposium on River, Coastal and Estuarine Morphodynamics*, 197–206. https://doi.org/10.13140/2.1.1562.5602

Blondeaux, P., & Vittori, G. (2010). Formation of tidal sand waves: Effects of the spring-neap cycle. *Journal of Geophysical Research: Oceans*, *115*(10), C10017, 1–7. https://doi.org/10.1029/2010JC006400

Blondeaux, P., & Vittori, G. (2011). The formation of tidal sand waves: Fully three-dimensional versus shallow water approaches. *Continental Shelf Research*, *31*(9), 990–996. https://doi.org/10.1016/j.csr.2011.03.005

Blondeaux, P., & Vittori, G. (2016). A model to predict the migration of sand waves in shallow tidal seas. *Continental Shelf Research*, *112*, 31–45. https://doi.org/10.1016/j.csr.2015.11.011

Blondeaux, P., & Vittori, G. (2022). Stability Analyses to Predict Tidal Sedimentary Patterns. In *50+ Years of AIMETA* (pp. 335–348). Springer International Publishing. https://doi.org/10.1007/978-3-030-94195-6_21

Bockelmann, F. D., Puls, W., Kleeberg, U., Müller, D., & Emeis, K. C. (2018). Mapping mud content and median grain-size of North Sea sediments – A geostatistical approach. *Marine Geology*, *397*, 60–71. https://doi.org/10.1016/j.margeo.2017.11.003

Bokuniewicz, H. J., Gordon, R. B., & Kastens, K. A. (1977). FORM AND MIGRATION OF SAND WAVES IN A LARGE ESTUARY, LONG ISLAND SOUND. *Marine Geology*, *24*, 185–199.

Borsje, B. W., de Vries, M. B., Bouma, T. J., Besio, G., Hulscher, S. J. M. H., & Herman, P. M. J. (2009a). Modeling bio-geomorphological influences for offshore sandwaves. *Continental Shelf Research*, *29*(9), 1289–1301. https://doi.org/10.1016/j.csr.2009.02.008

Borsje, B. W., Kranenburg, W. M., Roos, P. C., Matthieu, J., & Hulscher, S. J. M. H. (2014). The role of suspended load transport in the occurrence of tidal sand waves. *Journal of Geophysical Research: Earth Surface*, *119*(4), 701–716. https://doi.org/10.1002/2013JF002828

Borsje, B. W., Roos, P. C., Kranenburg, W. M., & Hulscher, S. J. M. H. (2013). Modeling tidal sand wave formation in a numerical shallow water model: The role of turbulence formulation. *Continental Shelf Research*, *60*, 17–27. https://doi.org/10.1016/j.csr.2013.04.023

Borsje, B. W., de Vries, M. B., Hulscher, S. J., & de Boer, G. J. (2008). Modeling large-scale cohesive sediment transport affected by small-scale biological activity. *Estuarine, Coastal and Shelf Science*, *78*(3), 468–480. https://doi.org/10.1016/j.ecss.2008.01.009

Borsje, B. W., Hulscher, S. J. M. H., Herman, P. M. J., & De Vries, M. B. (2009b). On the parameterization of biological influences on offshore sand wave dynamics. *Ocean Dynamics*, *59*(5), 659–670. https://doi.org/10.1007/s10236-009-0199-0

Campmans, G. H. P., Roos, P. C., de Vriend, H. J., & Hulscher, S. J. M. H. (2017). Modeling the influence of storms on sand wave formation: A linear stability approach. *Continental Shelf Research*, *137*, 103–116. https://doi.org/10.1016/j.csr.2017.02.002

Campmans, G. H. P., Roos, P. C., de Vriend, H. J., & Hulscher, S. J. M. H. (2018). The Influence of Storms on Sand Wave Evolution: A Nonlinear Idealized Modeling Approach. *Journal of Geophysical Research: Earth Surface*, *123*(9), 2070–2086. https://doi.org/10.1029/2018JF004616

Campmans, G. H. P., Roos, P. C., Van der Sleen, N. R., & Hulscher, S. J. M. H. (2021). Modeling tidal sand wave recovery after dredging: Effect of different types of dredging strategies. *Coastal Engineering*, *165*, 103862, 1–10. https://doi.org/10.1016/j.coastaleng.2021.103862

Campmans, G. H., van Dijk, T. A., Roos, P. C., & Hulscher, S. J. (2022). Calibration and Validation of Two Tidal Sand Wave Models: A Case Study of The Netherlands Continental Shelf. *Journal of Marine Science and Engineering*, *10*(12), 1902, 1–16. https://doi.org/10.3390/jmse10121902

Carniello, L., Defina, A., & D'Alpaos, L. (2012). Modeling sand-mud transport induced by tidal currents and wind waves in shallow microtidal basins: Application to the Venice Lagoon (Italy). *Estuarine, Coastal and Shelf Science*, *102–103*, 105–115. https://doi.org/10.1016/j.ecss.2012.03.016

Chen, D., Wang, Y., Melville, B., Asce, M., Huang, H., & Zhang, W. (2018). Unified Formula for Critical Shear Stress for Erosion of Sand, Mud, and Sand-Mud Mixtures. *Journal of Hydraulic Engineering*, *04018046*, 1–14. https://doi.org/10.1061/(ASCE)

Chen, D., Zheng, J., Zhang, C., Guan, D., Li, Y., & Wang, Y. (2021). Critical Shear Stress for Erosion of Sand-Mud Mixtures and Pure Mud. *Frontiers in Marine Science*, *8:713039*, 1–19. https://doi.org/10.3389/fmars.2021.713039

Cheng, C. H., Borsje, B. W., Beauchard, O., O'Flynn, S., Ysebaert, T., & Soetaert, K. (2021a). Small-scale macrobenthic community structure along asymmetrical sand waves in an underwater seascape. *Marine Ecology*, *42*(3), 1–15. https://doi.org/10.1111/maec.12657

Cheng, C. H., De Smit, J. C., Fivash, G. S., Hulscher, S. J. M. H., Borsje, B. W., & Soetaert, K. (2021b). Sediment shell-content diminishes current-driven sand ripple development and migration. *Earth Surface Dynamics*, *9*(5), 1335–1346. https://doi.org/10.5194/esurf-2021-13

Cheng, C. H., Soetaert, K., & Borsje, B. W. (2020). Sediment characteristics over asymmetrical tidal sand waves in the Dutch north sea. *Journal of Marine Science and Engineering*, *8*(6), 409, 1–16. https://doi.org/10.3390/JMSE8060409

Colina Alonso, A., van Maren, D. S., Herman, P. M., van Weerdenburg, R. J., Huismans, Y., Holthuijsen, S. J., Govers, L. L., Bijleveld, A. I., & Wang, Z. B. (2022). The Existence and Origin of Multiple Equilibria in Sand-Mud Sediment Beds. *Geophysical Research Letters*, *49*(22), 1–11. https://doi.org/10.1029/2022GL101141

Colina Alonso, A., Van Maren, D. S., Van Weerdenburg, R. J. A., Huismans, Y., & Wang, Z. B. (2023a). Improving morphodynamic modelling using sand-mud interaction and morphologic metrics. *NCK Days*, 26–26.

Colina Alonso, A., van Maren, D. S., van Weerdenburg, R. J. A., Huismans, Y., & Wang, Z. B. (2023b). Morphodynamic modelling of tidal basins: The role of sand-mud interaction. *Journal of Geophysical Research: Earth Surface*, *128*, 1–22. https://doi.org/10.1029/2023jf007391

Corenblit, D., Baas, A. C., Bornette, G., Darrozes, J., Delmotte, S., Francis, R. A., Gurnell, A. M., Julien, F., Naiman, R. J., & Steiger, J. (2011). Feedbacks between geomorphology and biota controlling Earth surface processes and landforms: A review of foundation concepts and current understandings. *Earth-Science Reviews*, *106*(3-4), 307–331. https://doi.org/10.1016/j.earscirev.2011.03.002

Creane, S., Coughlan, M., O'Shea, M., & Murphy, J. (2022). Development and Dynamics of Sediment Waves in a Complex Morphological and Tidal Dominant System: Southern Irish Sea. *Geosciences (Switzerland)*, *12*(12), 431, 1–46. https://doi.org/10.3390/geosciences12120431

Dabekaussen, W., Stam, J., Bakker, M. A. J., & Van Heteren, S. (2023). Zeebodemsedimentkaart voor het Nederlandse Continentaal Plat. Scale 1:200.000.

Damen, J. M., Van Dijk, T. A. G. P., & Hulscher, S. J. M. H. (2018). Spatially Varying Environmental Properties Controlling Observed Sand Wave Morphology. *Journal of Geophysical Research: Earth Surface*, *123*, 262–280. https://doi.org/10.4121/uuid:0d7e016d-2182-46ea-bc19-cdfda5c20308

Damveld, J. H., Borsje, B. W., Roos, P. C., & Hulscher, S. J. (2020a). Horizontal and Vertical Sediment Sorting in Tidal Sand Waves: Modeling the Finite-Amplitude Stage. *Journal of Geophysical Research: Earth Surface*, *125*(10), 1–20. https://doi.org/10.1029/2019JF005430

Damveld, J. H., van der Reijden, K. J., Cheng, C., Koop, L., Haaksma, L. R., Walsh, C. A. J., Soetaert, K., Borsje, B. W., Govers, L. L., Roos, P. C., Olff, H., & Hulscher, S. J. M. H. (2018). Video Transects Reveal That Tidal Sand Waves Affect the Spatial Distribution of Benthic Organisms and Sand Ripples. *Geophysical Research Letters*, *45*(21), 11, 837–11, 846. https://doi.org/10.1029/2018GL079858

Damveld, J. H. (2020). *The Feedbacks Among Tidal Sand Waves, Benthic Organisms and Sediment Sorting Processes* (Doctoral dissertation). University of Twente. Enschede.

Damveld, J. H., Borsje, B. W., Roos, P. C., & Hulscher, S. J. M. H. (2020b). Biogeomorphology in the marine landscape: Modelling the feedbacks between patches of the polychaete worm Lanice conchilega and tidal sand waves. *Earth Surface Processes and Landforms*, *45*(11), 2572–2587. https://doi.org/10.1002/esp.4914

Damveld, J. H., Roos, P. C., Borsje, B. W., & Hulscher, S. J. M. H. (2019). Modelling the two-way coupling of tidal sand waves and benthic organisms: A linear stability approach. *Environmental Fluid Mechanics*, *19*(5), 1073–1103. https://doi.org/10.1007/s10652-019-09673-1

De Jong, M. F., Baptist, M. J., Lindeboom, H. J., & Hoekstra, P. (2015). Relationships between macrozoobenthos and habitat characteristics in an intensively used area of the Dutch coastal zone. *ICES Journal of Marine Science*, *72*(8), 2409–2422. https://doi.org/10.1093/icesjms/fsv060

de Jong, M. F., Baptist, M. J., Lindeboom, H. J., & Hoekstra, P. (2015). Short-term impact of deep sand extraction and ecosystem-based landscaping on macrozoobenthos and sediment characteristics. *Marine Pollution Bulletin*, *97*(1-2), 294–308. https://doi.org/10.1016/j.marpolbul.2015.06.002

De Jong, M. F., Baptist, M. J., van Hal, R., de Boois, I. J., Lindeboom, H. J., & Hoekstra, P. (2014). Impact on demersal fish of a large-scale and deep sand extraction site with ecosystem-based landscaped sandbars. *Estuarine, Coastal and Shelf Science*, *146*, 83–94. https://doi.org/10.1016/j.ecss.2014.05.029

de Jong, M. F., Borsje, B. W., Baptist, M. J., van der Wal, J. T., Lindeboom, H. J., & Hoekstra, P. (2016). Ecosystem-based design rules for marine sand extraction sites. *Ecological Engineering*, *87*, 271–280. https://doi.org/10.1016/j.ecoleng.2015.11.053

Deltacommissie. (2008). *Samen werken met water: Een land dat leeft, bouwt aan zijn toekomst.*

Deltares. (2023). *Delft3D 3D/2D modelling suite for integral water solutions User Manual* (4.05).

Dodd, N., Blondeaux, P., Calvete, D., De Swart, H. E., Falqués, A., Hulscher, S. J. M. H., Różyński, G., & Vittori, G. (2003). Understanding Coastal Morphodynamics Using Stability Methods. *Journal of Coastal Research*, *19*(4), 849–865.

Duran Vinent, O., Andreotti, B., Claudin, P., & Winter, C. (2019). A unified model of ripples and dunes in water and planetary environments. *Nature Geoscience*, *12*(5), 345–350. https://doi.org/10.1038/s41561-019-0336-4

Durand, N., Tassi, P., Blanpain, O., & Lefebvre, A. (2023). Understanding marine dune dynamics in a shallow shelf sea using sediment mobility indices. In A. Valance, T. Garlan, A. Crave, & A. Gangloff (Eds.), *MARID VII. Seventh International Conference on Marine and River Dune Dynamics* (pp. 109–116). University of Rennes 1 and SHOM.

Exner, F. M. (1925). Über die Wechselwirkung zwischen Wasser un Geschiebe in Flüssen. *Sitzungsberichte Akademie der Wissenschaften in Wien Mathematisch-Naturwissenschatfliche Klasse, Abteilung 2a*, *134*, 165–180.

Folk, R. L. (1954). The Distinction between Grain Size and Mineral Composition in Sedimentary-Rock Nomenclature. *The Journal of Geology*, *62*(4), 344–359.

Gerkema, T. (2000). A linear stability analysis of tidally generated sand waves. *Journal of Fluid Mechanics*, *417*, 303–322. https://doi.org/10.1017/S0022112000001105

González, M., Medina, R., Espejo, A., Tintoré, J., Martin, D., & Orfila, A. (2010). Morphodynamic evolution of dredged sandpits. *Journal of Coastal Research*, *26*(3), 485–502. https://doi.org/10.2112/08-1034.1

Haasnoot, M., Bouwer, L., Diermanse, F., Kwadijk, J., Van der Spek, A., Oude Essink, G., Delsman, J., Weiler, O., Mens, M., Ter Maat, J., Van der Kaaij, T., Plieger, R., Huismans, Y., Sloff, K., Mosselman, E., & Lenselink, G. (2018). *Mogelijke gevolgen van versnelde zeespiegelstijging voor het Deltaprogramma: Een verkenning* (tech. rep. No. 11202230-005-0002). Deltares report. Delft.

Hendriks, E., van Prooijen, B. C., Aarninkhof, S. G. J., & Winterwerp, J. C. (2020). How human activities affect the fine sediment distribution in the Dutch Coastal Zone seabed. *Geomorphology*, *367*, 107314, 1–17. https://doi.org/10.1016/j.geomorph.2020.107314

Hendriks, E., van Prooijen, B. C., Cheng, C. H., Aarninkhof, S. G., Winterwerp, J. C., & Soetaert, K. E. (2022). An explanatory model for the burial of fines in the sandy seabed of the southern North Sea. *Marine Geology*, *454*, 106953, 1–18. https://doi.org/10.1016/j.margeo.2022.106953

Hendriks, E., Van Prooijen, B., Aarninkhof, S., Soetaert, K., & Winterwerp, H. (2019). Feedbacks between Fine-Grained Sediment Deposits and Bedforms in a Predominantly Sandy Seabed: Field Observations from the Southern North Sea. *Geophysical Research Abstracts*, *21*(EGU2019-13870).

Hirano, M. (1971). River bed degradation with armouring. *Japan Society of Civil Engineers*, *3*, 194–195.

Houbolt, J. J. H. C. (1968). Recent Sediments in the Southern Bight of the North Sea. *Geologie en Mijnbouw*, *47*(4), 245–273.

Hulscher, S. J. M. H. (1996). Tidal-induced large-scale regular bed form patterns in a three-dimensional shallow water model. *Journal of Geophysical Research: Oceans*, *101*(C9), 20727–20744. https://doi.org/10.1029/96JC01662

Hulscher, S. J. M. H., De Swart, H. E., & De Vriendt, H. J. (1993). The generation of offshore tidal sand banks and sand waves. *Continental Shelf Research*, *13*(11), 1183–1204.

Hulscher, S. J. M. H., & Van Den Brink, G. M. (2001). Comparison between predicted and observed sand waves and sand banks in the North Sea. *Journal of Geophysical Research: Oceans*, *106*(C5), 9327–9338. https://doi.org/10.1029/2001jc900003

Huthnance, J. M. (1982a). On One Mechanism Forming Linear Sand Banks. *Estuarine, Coastal and Shelf Science*, *14*, 79–99.

Huthnance, J. M. (1982b). On the Formation of Sand Banks of Finite Extent. *Estuarine, Coastal and Shelf Science*, *15*, 277–299.

IDON. (2011). *Integraal Beheerplan Noordzee 2015 Herziening*. Report DN0811VH11017.

Jacobs, W., Le Hir, P., Van Kesteren, W., & Cann, P. (2011). Erosion threshold of sand-mud mixtures. *Continental Shelf Research*, *31*(10), S14–S25. https://doi.org/10.1016/j.csr.2010.05.012

Jarvis, P. A., Bacik, K. A., Narteau, C., & Vriend, N. M. (2022). Coarsening Dynamics of 2D Subaqueous Dunes. *Journal of Geophysical Research: Earth Surface*, *127*(2). https://doi.org/10.1029/2021JF006492

Jones, C. G., Lawton, J. H., & Shachak, M. (1994). Organisms as Ecosystem Engineers. *Oikos*, *69*(3), 373–386.

Komarova, N. L., & Hulscher, S. J. M. H. (2000). Linear instability mechanisms for sand wave formation. *Journal of Fluid Mechanics*, *413*, 219–246. https://doi.org/10.1017/S0022112000008429

Kooistra, T. J., Witbaard, R., Soetaert, K., Bouma, T. J., & Pearson, S. G. (2023). How SANDsitive are seafloor animals in the Wadden Sea? Quantifying sandification sensitivity of Wadden Sea benthic communities. *NCK Days*, 72–72.

Krabbendam, J. M., Roche, M., Van Lancker, V. R. M., Nnafie, A., Terseleer, N., Degrendele, K., & De Swart, H. E. (2022). Do tidal sand waves always regenerate after dredging? *Marine Geology*, *451*, 1–8. https://doi.org/10.1016/j.margeo.2022.106866

Krabbendam, J. M., Nnafie, A., de Swart, H. E., Borsje, B. W., & Perk, L. (2021). Modelling the past and future evolution of tidal sand waves. *Journal of Marine Science and Engineering*, *9*(10), 1071, 1–21. https://doi.org/10.3390/jmse9101071

Krämer, K., Becker, M., & Winter, C. (2023). Bedform Transition in a Sediment Starved Environment (SW Baltic Sea). In A. Valance, T. Garlan, A. Crave, & A. Gangloff (Eds.), *MARID VII. Seventh International Conference on Marine and River Dune Dynamics* (pp. 141–147). University of Rennes 1 and SHOM.

Le Hir, P., Monbet, Y., & Orvain, F. (2007). Sediment erodability in sediment transport modelling: Can we account for biota effects? *Continental Shelf Research*, *27*(8), 1116–1142. https://doi.org/10.1016/j.csr.2005.11.016

Le Hir, P., Ficht, A., Silva Jacinto, R., Lesueur, P., Dupont, J. P., Lafite, R., Brenon, I., Thouvenin, B., & Cugier, P. (2001). Fine Sediment Transport and Accumulations at the Mouth of the. *Estuaries*, *24*(6B), 950–963.

Le Hir, P., Cann, P., Waeles, B., Hervé, J., & Bassoullet, P. (2005). Sediment and Ecohydraulics: 1NTERCOH 2005 Chapter 11 Erodibility of natural sediments: Experiments on sand/mud mixtures from laboratory and field erosion tests. In T. Kusuda, H. Yamanishi, J. Spearman, & J. Gailani (Eds.), *Sediment and Ecohydraulics: INTERCOH 2005* (pp. 137–153).

Le Hir, P., Cayocca, F., & Waeles, B. (2011). Dynamics of sand and mud mixtures: A multiprocess-based modelling strategy. *Continental Shelf Research*, *31*, S135–S149. https://doi.org/10.1016/j.csr.2010.12.009

Leenders, S., Damveld, J. H., Schouten, J., Hoekstra, R., Roetert, T. J., & Borsje, B. W. (2021). Numerical modelling of the migration direction of tidal sand waves over sand banks. *Coastal Engineering*, *163*, 103790, 1–15. https://doi.org/10.1016/j.coastaleng.2020.103790

Lokin, L. R., Warmink, J. J., & Hulscher, S. J. M. H. (2023). The influence of sediment transport formulae on modelling river dune development. In A. Valance, T. Garlan, A. Crave, & A. Gangloff (Eds.), *MARID VII. Seventh International Conference on Marine and River Dune Dynamics* (pp. 177–182). University of Rennes 1 and SHOM.

Mengual, B., Hir, P. L., Cayocca, F., & Garlan, T. (2017). Modelling fine sediment dynamics: Towards a common erosion law for fine sand, mud and mixtures. *Water*, *9*(8), 1–24. https://doi.org/10.3390/w9080564

Meysman, F. J., Middelburg, J. J., & Heip, C. H. (2006). Bioturbation: A fresh look at Darwin's last idea. *Trends in Ecology and Evolution*, *21*(12), 688–695. https://doi.org/10.1016/j.tree.2006.08.002

Mielck, F., Hass, H. C., Michaelis, R., Sander, L., Papenmeier, S., & Wiltshire, K. H. (2019). Morphological changes due to marine aggregate extraction for beach nourishment in the German Bight (SE North Sea). *Geo-Marine Letters*, *39*(1), 47–58. https://doi.org/10.1007/s00367-018-0556-4

Ministerie van Infrastructuur en Milieu & Ministerie van Economische Zaken. (2014). *Beleidsnota Noordzee 2016-2021*.

Ministerie van Infrastructuur en Waterstaat, Ministerie van Landbouw. Natuur en Voedselveiligheid, Ministerie van Economische Zaken en Klimaat, & Ministerie van Binnenlandse Zaken en Koninkrijksrelaties. (2022). *Programma Noordzee 2022-2027*.

Ministerie van Verkeer en Waterstaat, Ministerie van Volkshuisvesting Ruimtelijke Ordening en Milieubeheer, & Ministerie van Landbouw Natuur en Voedselkwaliteit. (2009). *Nationaal Waterplan 2009 - 2015*.

Mitchener, H., Torfs, H., & Whitehouse, R. (1996). Erosion of mud/sand mixtures. *Coastal Engineering*, *29*, 1–25.

Murray, J. M. H., Meadows, A., & Meadows, P. S. (2002). Biogeomorphological implications of microscale interactions between sediment geotechnics and marine benthos: A review. *Geomorphology*, *47*, 15–30.

Németh, A. A., Hulscher, S. J. M. H., & De Vriend, H. J. (2003). Offshore sand wave dynamics, engineering problems and future solutions. *Pipeline & Gas Journal*, *230*(4), 67–69.

Németh, A. A., Hulscher, S. J. M. H., & Van Damme, R. M. J. (2007). Modelling offshore sand wave evolution. *Continental Shelf Research*, *27*(5), 713–728. https://doi.org/10.1016/j.csr.2006.11.010

Németh, A. A., Hulscher, S. J. M. H., & De Vriend, H. J. (2002). Modelling sand wave migration in shallow shelf seas. *Continental Shelf Research*, *22*, 2795–2806.

Nnafie, A., Wolf, T. B., & de Swart, H. E. (2020). Tidal sand ridges on the shelf: A numerical study of their natural morphodynamic evolution and response to interventions. *Continental Shelf Research*, *205*, 104195, 1–16. https://doi.org/10.1016/j.csr.2020.104195

Overes, P. H. P., Borsje, B. W., Luijendijk, A. P., & Hulscher, S. J. M. H. (2023). Exploring the main drivers of sand wave dynamics. In A. Valance, T. Garlan, A. Crave, & A. Gangloff (Eds.), *MARID VII. Seventh International Conference on Marine and River Dune Dynamics* (pp. 231–237). University of Rennes 1 and SHOM.

Overes, P., Borsje, B., Luijendijk, A., & Hulscher, S. (2024). The importance of time-varying, non-tidal currents in modelling in-situ sand wave dynamics. *Coastal Engineering*. https://doi.org/10.1016/j.coastaleng.2024.104480

Paarlberg, A. J., Knaapen, M. A. F., De Vries, M. B., Hulscher, S. J. M. H., & Wang, Z. B. (2005). Biological influences on morphology and bed composition of an intertidal flat. *Estuarine, Coastal and Shelf Science*, *64*(4), 577–590. https://doi.org/10.1016/j.ecss.2005.04.008

Passchier, S., & Kleinhans, M. G. (2005). Observations of sand waves, megaripples, and hummocks in the Dutch coastal area and their relation to currents and combined flow conditions. *Journal of Geophysical Research: Earth Surface*, *110*(4), F04S15, 1–15. https://doi.org/10.1029/2004JF000215

Perera, C., Smith, J., Wu, W., Perkey, D., & Priestas, A. (2020). Erosion rate of sand and mud mixtures. *International Journal of Sediment Research*, *35*(6), 563–575. https://doi.org/10.1016/j.ijsrc.2020.06.004

Porcile, G., Blondeaux, P., & Vittori, G. (2017). On the formation of periodic sandy mounds. *Continental Shelf Research*, *145*, 68–79. https://doi.org/10.1016/j.csr.2017.07.011

Reiss, H., Cunze, H., König, K., Neumann, K., & Kröncke, I. (2011). Species distribution modelling of marine benthos: A North Sea case study. *Marine Ecology Progress Series*, *442*, 71–86. https://doi.org/10.3354/meps09391

Rijkswaterstaat. (2020). *Kustgenese 2.0: kennis voor een veilige kust*.

Roos, P. C., Blondeaux, P., Hulscher, S. J. M. H., & Vittori, G. (2005). Linear evolution of sandwave packets. *Journal of Geophysical Research: Earth Surface*, *110*(4), F04S14, 1–10. https://doi.org/10.1029/2004JF000196

Roos, P. C., Hulscher, S. J. M. H., Peters, B. G. T. M., & Németh, A. A. (2001). A Simple Morphodynamic Model for Sand Banks and Large-Scale Sand Pits Subject to Asymmetrical Tides. In S. Ikeda (Ed.), *River, Coastal and Estuarine Morphodynamics: RCEM 2001* (pp. 91–100).

Roos, P. C., & Hulscher, S. J. M. H. (2002). Formation of offshore tidal sand banks triggered by a gasmined bed subsidence. *Continental Shelf Research*, *22*, 2807–2818.

Roos, P. C., & Hulscher, S. J. M. H. (2003). Large-scale seabed dynamics in offshore morphology: Modeling human intervention. *Reviews of Geophysics*, *41*(2), 1010, 1–16. https://doi.org/10.1029/2002RG000120

Roos, P. C., Hulscher, S. J. M. H., & de Vriend, H. J. (2008). Modelling the morphodynamic impact of offshore sandpit geometries. *Coastal Engineering*, *55*(9), 704–715. https://doi.org/10.1016/j.coastaleng.2008.02.019

Roos, P. C., Hulscher, S. J. M. H., van der Meer, F. M., Dijk, T., Wientjes, I., & van den Berg, J. (2007). Grain size sorting over offshore sandwaves. In C. M. Dohmen-Janssen & S. J. M. H. Hulscher (Eds.), *River, Coastal and Estuarine Morphodynamics: RCEM 2007* (pp. 649–656). CRC Press. https://doi.org/10.1201/noe0415453639-c84

Salimi-Tarazouj, A., Hsu, T. J., Traykovski, P., & Chauchat, J. (2021). Eulerian Two-Phase Model Reveals the Importance of Wave Period in Ripple Evolution and Equilibrium Geometry. *Journal of Geophysical Research: Earth Surface*, *126*(7), 1–28. https://doi.org/10.1029/2021JF006132

Schandl, H., Fischer-Kowalski, M., West, J., & Giljum, S. (2016). *Global Material Flows and Resource Productivity. An Assessment Study of the UNEP International Resource Panel National Adaptation Policy Assessment View project MF-GLOBE-Developing multi-regional physical supply and use accounts for the analysis of global material and energy flows View project.*

Schindler, R. J., Parsons, D. R., Ye, L., Hope, J. A., Baas, J. H., Peakall, J., Manning, A. J., Aspden, R. J., Malarkey, J., Simmons, S., Paterson, D. M., Lichtman, I. D., Davies, A. G., Thorne, P. D., & Bass, S. J. (2015). Sticky stuff: Redefining bedform prediction in modern and ancient environments. *Geology*, *43*(5), 399–402. https://doi.org/10.1130/G36262.1

Seminara, G. (1995). Effect of grain sorting on the formation of bedforms. *Applied Mechanics Reviews*, *48*(9), 549–563.

Soulsby, R. L. (1997). *Dynamics of marine sands.* Thomas Telford.

Staatscourant. (2010). Beleidsregels Ontgrondingen in Rijkswateren. No. 14987.

Sterlini, F. M., Hulscher, S. J. M. H., & Hanes, D. M. (2009). Simulating and understanding sand wave variation: A case study of the Golden Gate sand waves. *Journal of Geophysical Research: Earth Surface*, *114*(2), F02007, 1–15. https://doi.org/10.1029/2008JF000999

Sterlini-van der Meer, F. M. (2009). *Modelling sand wave variation* (Doctoral dissertation). University of Twente. Enschede.

Svenson, C., Ernstsen, V. B., Winter, C., Bartholomä, A., & Hebbeln, D. (2009). Tide-driven Sediment Variations on a Large Compound Dune in the Jade Tidal Inlet Channel, Southeastern North Sea. *Journal of Coastal Research*, *SI56*, 361–365.

Sweco. (2017). *Winning suppletiezand Noordzee 2018 t/m 2027: Milieueffectrapportage* (tech. rep.).

Tonnon, P. K., van Rijn, L. C., & Walstra, D. J. R. (2007). The morphodynamic modelling of tidal sand waves on the shoreface. *Coastal Engineering*, *54*(4), 279–296. https://doi.org/10.1016/j.coastaleng.2006.08.005

UNEP. (2022). *Sand and Sustainability: 10 strategic recommendations to avert a crisis 2022. Grid-Geneva, United Nations Environment Programme.*

Van De Koppel, J., Herman, P. M., Thoolen, P., & Heip, C. H. (2001). Do alternate stable states occur in natural ecosystems? Evidence from a tidal flat. *Ecology*, *82*(12), 3449–3461. https://doi.org/10.1890/0012-9658(2001)082[3449:DASSOI]2.0.CO;2

van den Berg, J., Sterlini, F. M., Hulscher, S. J. M. H., & van Damme, R. M. J. (2012). Nonlinear process based modelling of offshore sand waves. *Continental Shelf Research*, *37*, 26–35. https://doi.org/10.1016/j.csr.2012.01.012

Van Der Meer, F. M., Hulscher, S. J. M. H., & Dodd, N. (2008). Modeling surface wave effects on evolved offshore sand waves. *14th Physics of Estuaries and Coastal Seas Conference, PECS 2008*, 187–190.

Van Der Meer, F. M., Hulscher, S. J. M. H., & Van Den Berg, J. (2007). On the influence of suspended sediment transport on the generation of offshore sand waves. In B. J. Geurts,

H. Clercx, & W. Uijttewaal (Eds.), *Particle Laden Flow: From Geophysical to Kolmogorov Scales* (pp. 29–41).

Van der Meijden, R., Damveld, J. H., Ecclestone, D. W., Van der Werf, J. J., & Roos, P. C. (2023). Shelf-wide analyses of sand wave migration using GIS: A case study on the Netherlands Continental Shelf. *Geomorphology*, *424*, 108559, 1–17. https://doi.org/10.1016/j.geomorph.2022.108559

Van Der Veen, H. H., Hulscher, S. J. M. H., & Knaapen, M. A. F. (2006). Grain size dependency in the occurrence of sand waves. *Ocean Dynamics*, *56*, 228–234. https://doi.org/10.1007/s10236-005-0049-7

Van Dijk, T. A., Van Dalfsen, J. A., Van Lancker, V., Van Overmeeren, R. A., Van Heteren, S., & Doornenbal, P. J. (2012). Benthic Habitat Variations Over Tidal Ridges, North Sea, The Netherlands. In *Seafloor Geomorphology as Benthic Habitat* (pp. 241–249). Elsevier Inc. https://doi.org/10.1016/B978-0-12-385140-6.00013-X

van Gerwen, W., Borsje, B. W., Damveld, J. H., & Hulscher, S. J. M. H. (2018). Modelling the effect of suspended load transport and tidal asymmetry on the equilibrium tidal sand wave height. *Coastal Engineering*, *136*, 56–64. https://doi.org/10.1016/j.coastaleng.2018.01.006

Van Ledden, M. (2001). *Modelling of sand-mud mixtures Part II: A process-based sand-mud model* (tech. rep.). WL — Delft Hydraulics. Delft.

Van Oyen, T., & Blondeaux, P. (2009a). Tidal sand wave formation: Influence of graded suspended sediment transport. *Journal of Geophysical Research: Oceans*, *114*, C07004, 1–18. https://doi.org/10.1029/2008JC005136

Van Oyen, T., & Blondeaux, P. (2009b). Grain sorting effects on the formation of tidal sand waves. *Journal of Fluid Mechanics*, *629*, 311–342. https://doi.org/10.1017/S0022112009006387

Van Oyen, T., Blondeaux, P., & Van den Eynde, D. (2013). Sediment sorting along tidal sand waves: A comparison between field observations and theoretical predictions. *Continental Shelf Research*, *63*, 23–33. https://doi.org/10.1016/j.csr.2013.04.005

Van Rijn, L. C. (2020). *LITERATURE REVIEW OF CRITICAL BED-SHEAR STRESSES FOR MUD-SAND MIXTURES* (tech. rep.).

van Santen, R. B., de Swart, H. E., & van Dijk, T. A. (2011). Sensitivity of tidal sand wavelength to environmental parameters: A combined data analysis and modelling approach. *Continental Shelf Research*, *31*(9), 966–978. https://doi.org/10.1016/j.csr.2011.03.003

Vittori, G., & Blondeaux, P. (2022). Predicting offshore tidal bedforms using stability methods. *Earth-Science Reviews*, *235*, 104234, 1–23. https://doi.org/10.1016/j.earscirev.2022.104234

Walgreen, M., de Swart, H. E., & Calvete, D. (2003). Effect of grain size sorting on the formation of shoreface-connected sand ridges. *Journal of Geophysical Research: Oceans*, *108*(3), 3063, 1–16. https://doi.org/10.1029/2002jc001435

Walgreen, M., De Swart, H. E., & Calvete, D. (2004). A model for grain-size sorting over tidal sand ridges. *Ocean Dynamics*, *54*, 374–384. https://doi.org/10.1007/s10236-003-0066-3

Wang, Z., Liang, B., Wu, G., & Borsje, B. W. (2019). Modeling the formation and migration of sand waves: The role of tidal forcing, sediment size and bed slope effects. *Continental Shelf Research*, *190*, 103986, 1–13. https://doi.org/10.1016/j.csr.2019.103986

Widdows, J., & Brinsley, M. (2002). Impact of biotic and abiotic processes on sediment dynamics and the consequences to the structure and functioning of the intertidal zone. *Journal of Sea Research*, *48*, 143–156.

Wientjes, I. G. M. (2006). *Grain size sorting over offshore sandwaves* (MSc Thesis). University of Twente. Enschede.

Witbaard, R., & Craeymeersch, J. (2023). *Littekens op de zeebodem. Een onderzoek naar de faunistische effecten op lange termijn van diepe zandwinning voor de Nederlandse kust* (tech. rep. No. 2023-01). Netherlands Institute for Sea Research (NIOZ). Texel. https://doi.org/10.25850/nioz/7b.b.8d

Wu, X., Malarkey, J., Fernández, F., Baas, J. H., & Parsons, D. R. (2023). Clay winnowing associated with wave-current ripple dynamics on cohesive sand-clay beds. In A. Valance, T. Garlan, A. Crave, & A. Gangloff (Eds.), *MARID VII. Seventh International Conference on Marine and River Dune Dynamics* (pp. 331–337). University of Rennes 1 and SHOM.

Yuan, B., de Swart, H. E., & Panadès, C. (2016). Sensitivity of growth characteristics of tidal sand ridges and long bed waves to formulations of bed shear stress, sand transport and tidal forcing: A numerical model study. *Continental Shelf Research*, *127*, 28–42. https://doi.org/10.1016/j.csr.2016.08.002

Yuan, B., de Swart, H. E., & Panadès, C. (2017). Modeling the finite-height behavior of offshore tidal sand ridges, a sensitivity study. *Continental Shelf Research*, *137*, 72–83. https://doi.org/10.1016/j.csr.2017.02.007